

## ***Recent explosive volcanism at the eastern Trans-Mexican Volcanic Belt***

**G. Carrasco-Núñez\***

**P. Dávila-Harris**

*Centro de Geociencias, Universidad Nacional Autónoma de México, Campus Juriquilla, Querétaro, Qro., 76230 Mexico*

**N.R. Riggs**

**M.H. Ort**

*School of Earth Sciences and Environmental Sustainability, Northern Arizona University, Flagstaff, Arizona, USA*

**B.W. Zimmer**

*Department of Geology, Appalachian State University, Boone, North Carolina USA*

**C.P. Willcox**

**M.J. Branney**

*Department of Geology, University of Leicester, Leicester, LE17RH, UK*

### **ABSTRACT**

**The eastern Trans-Mexican Volcanic Belt is characterized by a diversity of volcanoes that are related to different processes and eruptive styles. The spectacular exposures of late Pleistocene and Holocene volcanism provide a unique opportunity to explore a variety of volcanic features and deposits that may be relevant for volcanic hazard assessments within the area. This three-day field guide describes selected representative examples of the regional volcanism showing volcanic features including thick pyroclastic successions derived from the explosive activity of Los Humeros caldera volcano, caldera-rim effusions, alternating explosive and effusive activity of a vitrophyric rhyolite dome (Cerro Pizarro), and the eruptive activity of two compositionally contrasting maar volcanoes: Atexcac, a classic basaltic maar and Cerro Pinto, a rhyolitic tuff ring–dome complex.**

---

\*gerardoc@dragon.geociencias.unam.mx

Carrasco-Núñez, G., Dávila-Harris, P., Riggs, N.R., Ort, M.H., Zimmer, B.W., Willcox, C.P., and Branney, M.J., 2012, Recent explosive volcanism at the eastern Trans-Mexican Volcanic Belt, *in* Aranda-Gómez, J.J., Tolson, G., and Molina-Garza, R.S., eds., *The Southern Cordillera and Beyond: Geological Society of America Field Guide 25*, p. 83–113, doi:10.1130/2012.0025(05). For permission to copy, contact editing@geosociety.org. ©2012 The Geological Society of America. All rights reserved.

## INTRODUCTION

One focus of volcanology is the study of active volcanoes because active systems often pose hazards to local populations. Identifying that a volcano is active is just the first step. It is also important to consider the eruptive character of long-dormant volcanoes or volcanoes that have not been explored in detail, as these studies may result in the discovery of important considerations for hazard assessments. Therefore, we emphasize the importance of conducting detailed studies on recently active volcanoes to determine their evolution and eruptive history, including eruption frequency, styles, repose periods, and possible cyclicity, which may provide insights about the nature of possible future activity.

The purpose of this field guide is to describe a three-day itinerary to examine examples of recent (late Pleistocene and Holocene) volcanism in the eastern Trans-Mexican Volcanic Belt, where the diversity of volcanoes, coupled with spectacular exposures, provides a unique opportunity to explore a variety of volcanic features and deposits that may be relevant for volcanic hazard assessments within the area. Due to the short duration of the trip, we have selected outstanding volcanoes that have easy access.

We will examine the complex 0.5 Ma pyroclastic succession of Los Humeros caldera volcano, which records intense explosive events and caldera-rim effusions. We will also examine a vitrophyric rhyolite dome (Cerro Pizarro) that shows evidence of complex polygenetic behavior, and two contrasting maar volcanoes: Atexcac, a classic basaltic maar and Cerro Pinto, a tuff ring–dome complex. The locations of the volcanoes are shown in Figure 1. (Note that in Mexico, maars that produce dry craters are named *xalapaxcos*, a Nahuatl term meaning “vessel with sand,” whereas those craters with a crater lake are called *axalapaxcos*).

On Day 1 we shall drive 4.5 h to Perote, where we will stay overnight. Day 2 will be spent at Los Humeros caldera volcano, to examine the record of explosive activity during and between successive major caldera-forming events. We will compare the extra-caldera successions with the successions within the caldera and from the caldera rim. We will also discuss the eruptive potential of the active geothermal area and the threat it may pose to the area.

On Day 3, we will drive to the south of the Serdán-Oriental basin (Fig. 1) to explore different types of volcanoes, starting with Cerro Pizarro. We will examine the explosive and other volcanoclastic products associated with the construction and partial destruction of the Cerro Pizarro rhyolitic dome and the relation of these products to deposits derived from Los Humeros volcano. We will observe how an isolated rhyolitic dome, a volcano type usually regarded as monogenetic and short-lived (10s–100s years), is a polygenetic volcano with a complex evolution, involving long repose periods (~50–80 k.y.) between eruptions. This indicates that reawakening of an apparently extinct rhyolite dome cannot be entirely ruled out, even if the last explosive eruption occurred at 65 ka. We will then examine the complex stratigraphic relations at Cerro Pinto volcano, which reveal alternating periods of explosive and effusive activity at this tuff ring–

dome complex. Then we shall explore the internal structure of the basaltic Atexcac maar volcano, which records interactions with the country rock and vent migration. In contrast to many maars elsewhere (Lorenz, 1986), this example was subjected to a water influx at the end of the eruption sequence.

## REGIONAL GEOLOGIC SETTING

The Trans-Mexican Volcanic Belt is a Neogene to Holocene (Ferrari et al., 1999) seismically and volcanically active E–W–trending volcanic province. It extends more than 1000 km from the Pacific coast to the Gulf of Mexico (Fig. 1). Large stratovolcanoes are the most conspicuous feature of the landscape, but other types of volcanoes are also present, including several large caldera volcanoes, several rhyolite dome volcanoes, and thousands of maar volcanoes and scoria and lava cones. The magmas are mainly calc-alkaline and range from basalt to rhyolite. The province has several high-relief, nearly N–S–trending volcanic ranges formed by large stratovolcanoes, separated by wide intermontane lacustrine/playa basins. Fertile volcanic soil and a favorable climate have attracted people to central Mexico for millennia and this area continues to be the most populated region of the country. This population density is significant for volcanic hazard assessments.

The eastern Trans-Mexican Volcanic Belt comprises the Serdán-Oriental basin and the Cofre de Perote–Citlaltépetl volcanic range (Fig. 1). The volcanism is dominated by Quaternary volcanoes, although isolated Pliocene volcanoes are also present. Basement rocks and intrusive rocks are also exposed in the area (Yáñez and García, 1982), and the Serdán-Oriental basin is bounded to the west by abundant Miocene volcanics (Carrasco-Núñez et al., 1997).

### Basement and Intrusive Rocks

The regional basement of the eastern Trans-Mexican Volcanic Belt comprises highly deformed Cretaceous limestone and shale that rest on a Paleozoic crystalline basement, exposed in the Teziutlán massif, northeast of Los Humeros volcano (Viniegra, 1965). These basement rocks form a  $\leq 3000$ -m-thick conspicuous NW–trending folded and faulted mountain range. The basement is intruded by small Oligocene and Miocene small plutons of granodiorite, monzonite and syenite (Yáñez and García, 1982). The oldest exposed volcanic rocks are andesitic and ferrobaltic lava (dated at 3.5 Ma, Yáñez and García, 1982, and 1.55 Ma, Ferriz and Mahood, 1984). Volcanism in the Serdán-Oriental basin has been active since Pliocene time, but in the surrounding areas since the Miocene epoch (Yáñez and García, 1982; Carrasco-Núñez et al., 1997; Gómez-Tuena and Carrasco-Núñez, 2000).

### Serdán-Oriental Basin

The Serdán-Oriental basin is a broad (5250 km<sup>2</sup>), internally drained, intermontane basin of the Mexican Altiplano, with an

average elevation of 2300 masl. The basin is characterized by monogenetic bimodal volcanism that has produced scattered rhyolitic domes and smaller, isolated cinder, scoria, and lava cones of basaltic composition, and some maar volcanoes, tuff rings, and tuff cones (see Yáñez and García, 1982, and Negendank et al., 1985, for an overview). The Serdán-Oriental basin is bounded to the north by Los Humeros volcano, a quasi-circular, ~20-km-diameter Pleistocene silicic caldera volcano. Two voluminous

ignimbrites emplaced at ca. 0.46 Ma (Ferriz and Mahood, 1984) and ca. 0.14 Ma (Willcox, 2011) are widely distributed and cover most of the northern part of the Serdán-Oriental basin. To the east, the Sierra Negra–Citlaltépetl–Cofre de Perote range (Fig. 1) of Quaternary andesitic stratovolcanoes forms a marked topographic divide that separates the High Plain from the Gulf of Mexico coastal plain. To the south lies a range of highly folded and faulted Mesozoic sedimentary rocks. To the west are the

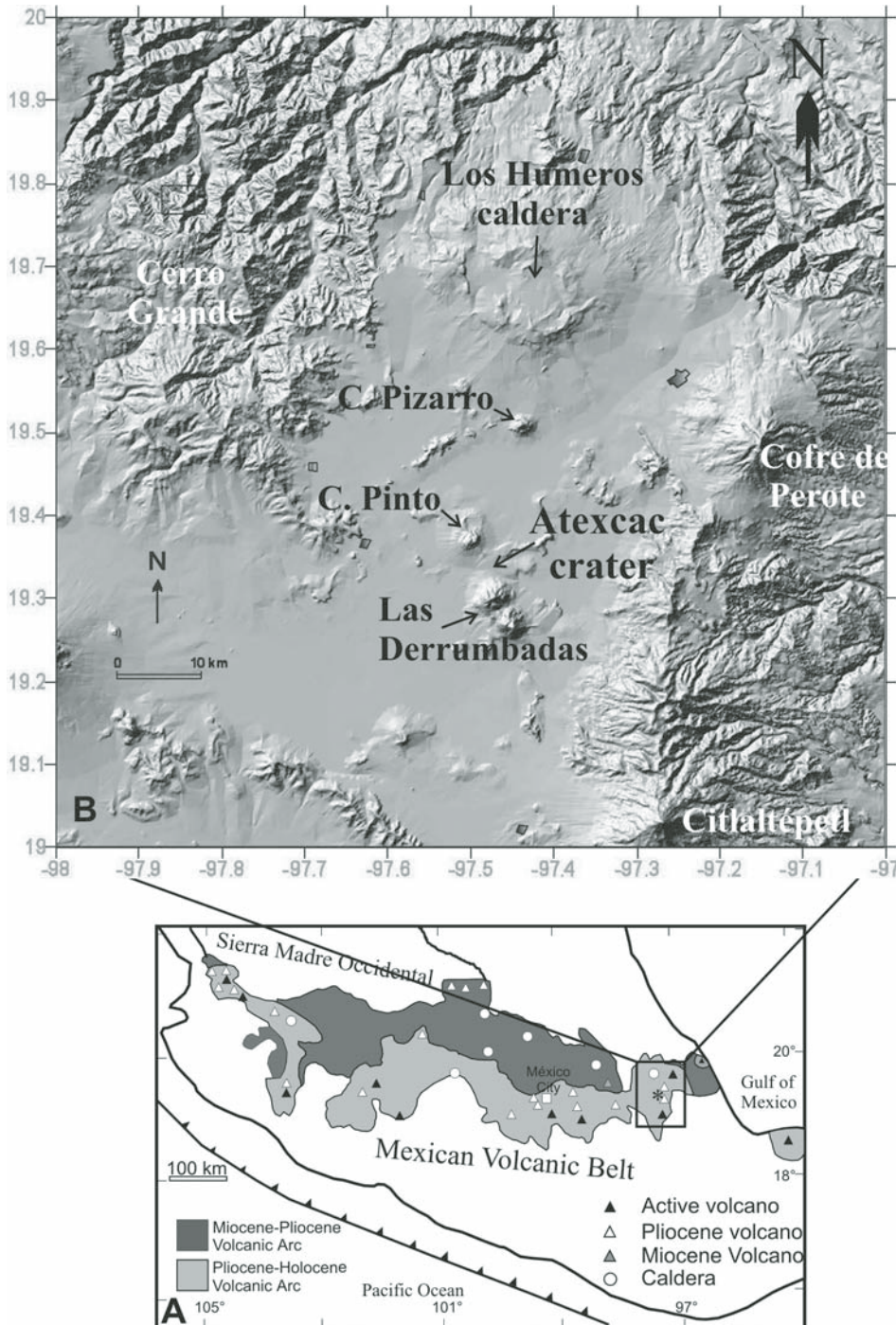


Figure 1. Location of the field trip area in the eastern Trans-Mexican Volcanic Belt (A), and digital elevation model showing the morphology and distribution of the main volcanoes to be explored in the field trip, including Los Humeros caldera, Cerro Pizarro rhyolitic dome, Cerro Pinto tuff ring-dome complex and Atexcac maar (B).

Miocene andesitic Cerro Grande volcano and the Pleistocene andesitic-dacitic La Malinche stratovolcano.

About a dozen maar volcanoes occur in the Serdán-Oriental Basin, with compositions from basalt to rhyolite (Ordóñez, 1905, 1906; Gasca-Durán, 1981). The maars have circular, elliptical and irregularly shaped craters, and some contain a crater lake. These volcanoes have been described in general by Siebe *et al.* (1995)<sup>1</sup>, and some have been described individually, such as the multiple-vent Cerro Xalapaxco tuff cone (Abrams and Siebe, 1994) and the Tepexitl tuff ring, a shallow rhyolitic xalapaxco (Austin-Erickson, 2007; Austin-Erickson *et al.*, 2011), and Tecuitlapa maar (Ort and Carrasco-Núñez, 2009). Others, such as Alchichica or Aljojuca, have not yet been investigated in detail. Some of the cinder cones are aligned in E-W or ENE-WSW orientations, particularly in the south. This pattern is similar to the central Trans-Mexican Volcanic Belt, where this trend reflects the dominant regional stress direction.

### Cofre de Perote-Citlaltépetl Volcanic Range

The Cofre de Perote–Citlaltépetl range comprises large andesitic-dacitic composite volcanoes, including, from south to north, the presently dormant Citlaltépetl (also called Pico de Orizaba) stratovolcano (Carrasco-Núñez, 2000), followed by Las Cumbres (Rodríguez-Elizarrarás, 2005) and la Gloria complexes and the shield-like compound Cofre de Perote (Carrasco-Núñez *et al.*, 2010) (Fig. 1).

The Cofre de Perote–Citlaltépetl volcanic range forms an important physiographical divide separating the Altiplano (Serdán-Oriental basin) to the west from the Gulf Coastal Plain to the east. Its substrate slopes eastward, and this has facilitated repeated flank collapses of the volcanoes toward the Gulf Coastal Plain (Carrasco-Núñez *et al.*, 2006). The two sides of the volcanic range have contrasting climatic conditions and drainages: the Gulf Coastal Plain has a well-developed, integrated drainage network of deeply incised gullies, due to the very high rates of precipitation, whereas the Serdán-Oriental basin has an arid climate, has no integrated drainage network, and is dominated by ephemeral streams, shallow lakes, and salt pans.

Current volcanic activity within the eastern Trans-Mexican Volcanic Belt is restricted to the dormant Citlaltépetl (Pico de Orizaba) stratovolcano, which today shows passive fumarolic activity. Very recent (pre-Columbian) activity at El Volcancillo at the northern end of the belt is indicated by recent stratigraphic studies (Siebert and Carrasco-Núñez, 2002). El Volcancillo is a paired scoria cone that erupted as recently as ca. 900 yr B.P., and is located at the end of an ENE cone alignment parallel to a regional seismically active structural system (Siebert and Carrasco-Núñez, 2002). Although the Cofre de Perote com-

plex can be regarded as extinct, several edifice collapses have occurred since late Pleistocene-Holocene time that have significant hazards implications (Carrasco-Núñez *et al.*, 2010).

## RECENT VOLCANISM OF THE SERDÁN-ORIENTAL BASIN

### Los Humeros Caldera

#### Definition

Los Humeros volcano is one of the largest caldera volcanoes in central Mexico and hosts one of the most important geothermal fields in the country, producing ~45 Mw of power. Los Humeros is the northernmost volcano of the Serdán-Oriental basin and lies west of andesitic stratovolcanoes of the Citlaltépetl–Cofre de Perote range (Fig. 1). Los Humeros comprises at least two calderas: a smaller (9 km diameter) structure known as Los Potreros caldera lies nested within the larger (21 × 15 km diameter) Los Humeros caldera. Although the two caldera-forming eruptions were large, involving 15 km<sup>3</sup> (Carrasco-Núñez and Branney, 2005; Willcox, 2011) and 115 km<sup>3</sup> (Ferriz and Mahood, 1984) dense rock equivalent (DRE), respectively, its most recent activity (younger than 20 ka) is dominated by ring-fracture basaltic lava flows. The geothermal field is apparently controlled by a NW-trending structural system, as inferred from stratigraphy derived from borehole data (Cedillo, 1997).

#### Evolution

The evolution of Los Humeros volcano (Fig. 2) began at ca. 0.5 Ma and includes at least 32 pyroclastic eruptions, including two major silicic ignimbrite-forming eruptions and numerous plinian eruptions, interspersed with dacitic and rhyodacitic dome-forming eruptions and, most recently, ring-fracture volcanism dominated by basaltic and basaltic-andesite lava flows and minor strombolian activity (Ferriz and Mahood, 1984; Willcox, 2011). At least three main stages can be recognized, each involving large explosive eruptions. During the first stage, precaldera high-silica rhyolite lavas erupted from several vents were disrupted by a caldera-forming explosive eruption at ca. 460 ka that formed the 21 km × 15 km Los Humeros caldera. Pyroclastic density currents from this eruption emplaced the Xáltipan ignimbrite, a 115 km<sup>3</sup> (DRE) the high-silica rhyolite ignimbrite, which is widely distributed radially from source.

During the second stage (ca. 360 ka to 140 ka), several high-silica rhyolite domes were emplaced within the caldera and along its rim, culminating with a series of plinian and sub-plinian explosive eruptions that produced >10 km<sup>3</sup> (DRE) of rhyodacitic-andesitic pumice fallout layers known collectively as the Faby Formation (Ferriz and Mahood, 1984; Willcox, 2011).

The third stage (60–100 ka) was marked by the 15 km<sup>3</sup> (DRE) eruption of the predominantly rhyodacitic Zaragoza ignimbrite (Carrasco-Núñez and Branney, 2005; Carrasco-Núñez *et al.*, 2012), accompanied by subsidence of the quasi-circular, 9-km-diameter Los Potreros caldera, nested within Los Humeros

GSA Data Repository item 2012084, "Quaternary explosive volcanism and pyroclastic deposits in east central Mexico: implications for future hazards" by Siebe *et al.* (1995), is available at <http://www.geosociety.org/pubs/ft2012.htm>, or on request from [editing@geosociety.org](mailto:editing@geosociety.org).

caldera. The general distribution of the Zaragoza ignimbrite is shown in Figure 3C. Several plinian eruptions (Rosa and Yerba formations; Willcox, 2011) followed, including a  $>0.34 \text{ km}^3$  (DRE) dacitic pumice fall deposit (Xoxoctic Member;  $>65 \text{ ka}$ );  $\sim 6 \text{ km}^3$  of andesitic and basaltic andesite lavas and scoria cones (40 and 30 ka); and the eruption of about  $\sim 1 \text{ km}^3$  of rhyodacitic and andesitic tephra (Cuicuiltic Member; Willcox, 2011). The 1.7-km-diameter El Xalapaxco caldera may have subsided during this stage. The most recent volcanic activity was the 20 ka effusion of  $\sim 0.25 \text{ km}^3$  of olivine basalt lava flows from the southern margin of Los Humeros caldera (Fig. 3D). Recent studies indicate that the most recent volcanism is Holocene.

### Faby Formation

The Faby Formation (Willcox, 2011; “Faby Tuff” of Ferriz and Mahood, 1984) is a succession of 15 andesitic to rhyolitic plinian pumice fall layers, two volcanoclastic sedimentary units and a rhyolite lava erupted during a period of ca. 160 ka, with a quarry type locality  $\sim 3 \text{ km}$  southeast of Los Humeros caldera and 2.5 km north of El Frijol Colorado, near Stop 1. The base of the

formation is marked by the first eruption unit (Perote Member), which overlies the older and more altered Humeros Formation (Willcox, 2011). The upper contact of the Faby Formation is seen in the center of the eastern wall of Los Potrerros caldera, where the overlying Potrerros Formation overlies caldera lake sediments (probably the youngest pre-Zaragoza deposit).

The three geographically separate pyroclastic successions in the Faby Formation do not interfinger but are constrained by overlying or underlying units dated by  $^{40}\text{Ar}$ - $^{39}\text{Ar}$  (Willcox, 2011). Most of the deposits were emplaced to the east, southeast and south of the caldera, indicating the prevailing paleowind directions to the SE.

### Cuicuiltic Member

The Cuicuiltic Member (Willcox, 2011; “Cuicuiltic Tuff” of Ferriz and Mahood, 1984) was originally described as a “visually striking sequence of interbedded rhyodacitic and andesitic air-fall lapilli tuffs,” apparently representing  $0.1 \text{ km}^3$  of erupted magma that was related to subsidence of the El Xalapaxco collapse structure (Ferriz and Mahood, 1984; Fig. 3C). The Cuicuiltic eruption is now regarded as a far more complex event involving at least three simultaneously active vents, one a subplinian eruption of rhyodacite pumice and the other two or more being Strombolian fissure eruptions along reactivated caldera faults (Dávila-Harris and Carrasco-Núñez, 2010). New stratigraphic and isopach data (Dávila-Harris and Carrasco-Núñez, unpublished data) do not support the idea that the Xalapaxco crater was the eruptive source.

The Cuicuiltic Member is exposed widely within the caldera, and to a lesser extent on the southern flank of the caldera. It drapes most fault scarps and smooth hills within the caldera because it is one of the youngest pyroclastic deposits at the volcano (ca. 30 ka). At most places it overlies a brown paleosol. Around Los Potrerros, it lies on a thin paleosol developed on a lithic-rich ignimbrite and scoria agglomerates. It also rests unconformably on the Zaragoza Ignimbrite and over the Xoxoctic Member (“Xoxoctic Tuff” of Ferriz and Mahood, 1984). To the north and northwest of the caldera, the Cuicuiltic Member unconformably drapes older lava fields and undifferentiated, phreatomagmatic pyroclastic deposits and to the northwest it unconformably overlies the glassy Oyameles rhyolite dome, which post-dates the Xáltipan ignimbrite. On the southern flank it overlies agglomeratic scorias and rests unconformably on Faby Member plinian pumice-fall deposits.

The Cuicuiltic Member has been subdivided into nine units (C1–C9) on the basis of textural and chemical characteristics. The lower units, C1 and C2, contain white, highly inflated trachydacite pumice lapilli. C3 contains both rhyodacite and mingled pumice. Layers C4 and C6 consist of basaltic-andesite dense pumice and scoria lapilli and blocks. C5 lies between these two mafic units and comprises a thin layer of white to gray, coarse-ash to fine lapilli. Units C7, C8, and C9 are widely varied. C7 is a mixture of white trachydacite pumice, scoria lapilli, and banded pumice;

Summary of Los Humeros caldera geology (modified from Ferriz and Mahood, 1984)		
Ma	Eruptive event	Volume (km <sup>3</sup> )
<0.02	Olivine basaltic lavas	0.25
0.02	Rhyodacitic and andesitic lavas	10
	Eruption of rhyodacitic and andesitic pumice fall (Cuicuiltic tuff) & formation of El Xalapaxco caldera	1
0.03-0.04	Peripheral Scoria cones and andesite lavas	6
0.05	Explosive eruption producing the Xoxoctic Tuff	0.6
~ 0.1	Eruption of the Zaragoza Ignimbrite & formation of Los Potrerros caldera	12
0.24	Plinian pumice-fall eruption (Faby Tuff)	10
	Ring-fracture rhyolite lavas	
0.36	Eruption of rhyolitic domes	4.7
0.46	Eruption of the Xáltipan Ignimbrite formation of Los Humeros caldera	115

Figure 2. Summary of the geological evolution of Los Humeros caldera from Ferriz and Mahood (1984), including the age of the most important eruptive events (left column) and the estimated volume for each event (right-hand column)

C8 is made up of pumice and scoria blocks with rare white and banded pumice; and C9 is of brown to gray andesitic pumice.

The importance of the Cuicuilt Member lies within its eruption mechanisms and the previously unknown recent age of the event, ca. 30 ka. Unknown processes at depth caused the felsic magma (represented by C1 and C2) to reactivate faults and to erupt simultaneously with basic vents along these reactivated faults. The common explanation invoked for the emplacement of chemically zoned volcanic deposits suggests that small mafic intrusions trigger explosive eruptions of differentiated, stratified

magma chambers. Evidence includes mingled pumice and stratigraphic variations of trace and major elements, and examples of this include the Zaragoza Ignimbrite (Carrasco-Núñez and Branney, 2005; this guide), the Granadilla and Poris Formations in Tenerife (Bryan *et al.*, 1998; Brown and Branney, 2004) and many others. In contrast, in the Cuicuilt eruption, the basaltic-andesite products were erupted from laterally independent satellite vents (at least three, represented by C4, C6, and C8, as revealed from stratigraphic and isopach and isopleth maps; Dávila-Harris and Carrasco-Núñez, unpublished data). The features within these

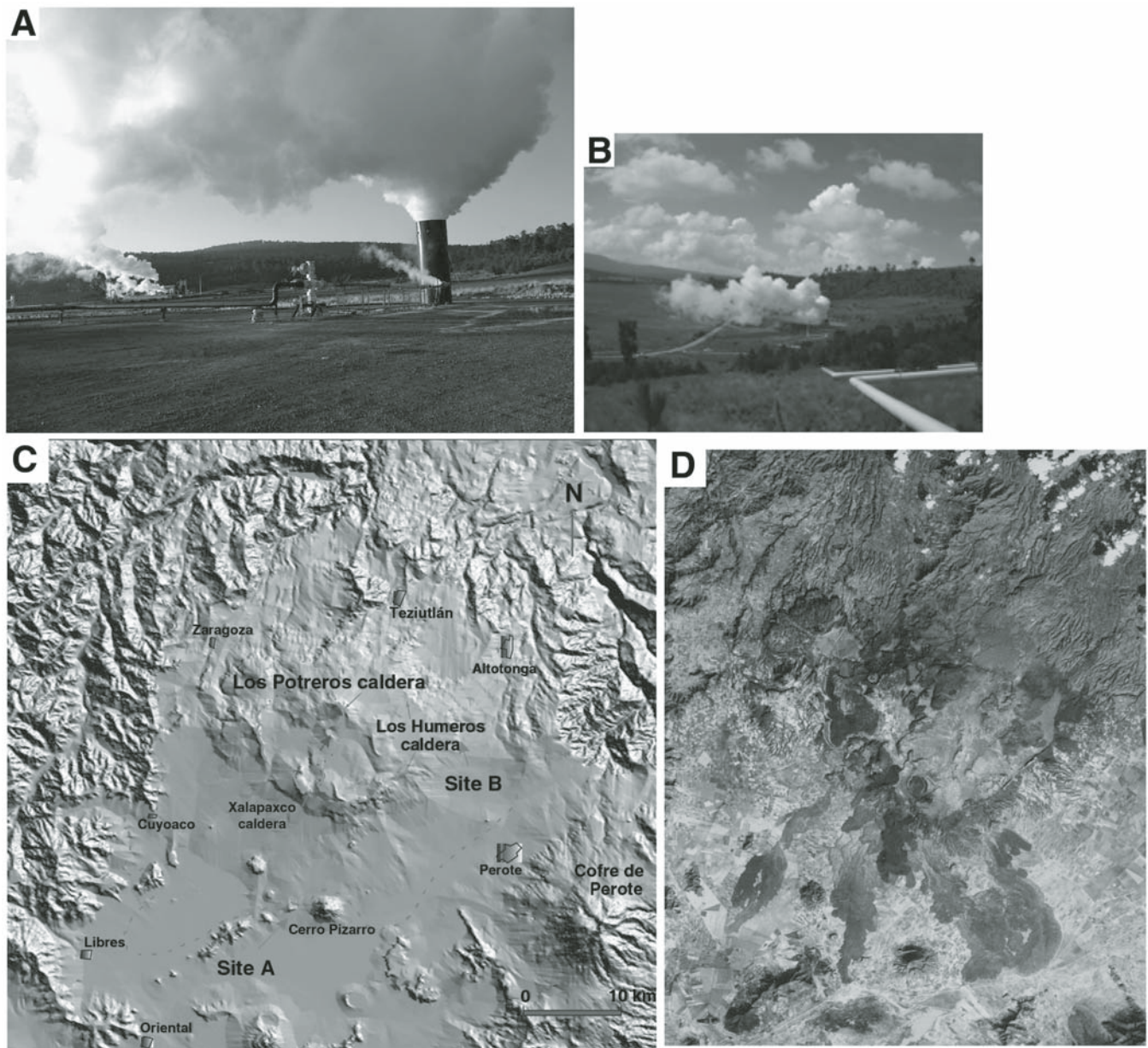


Figure 3. (A, B) Active wells within Los Humeros geothermal field. (C) Distribution of the Zaragoza ignimbrite and structures defining the caldera rims of Los Potreros and Humeros calderas. Sites A and B indicate the type sections; B is the site of Stop 7. (D) Landsat Thematic Mapper false-color image showing the structures of Los Humeros caldera and distribution of Late Pleistocene caldera-rim lava flows.

units suggest the existence of separate vents acting simultaneously, while for other units (C3, C7, and C9), mingling and efficient mixture of magma is recorded within the juvenile material. Magma mixing may be due to a zoned magma chamber or an intrusion of a mafic body.

### Zaragoza Ignimbrite

The second largest explosive eruption from Los Humeros caldera is recorded by the Zaragoza Member (Willcox, 2011; “Zaragoza tuff” of Ferriz and Mahood, 1984). The Zaragoza ignimbrite comprises two plinian pumice-fall layers with an intraplinian compound ignimbrite, the Zaragoza ignimbrite. The ignimbrite is non-welded, non-indurated and comprises predominantly massive, poorly sorted lapilli and ash. It has several minor flow units, mostly near the base, and a thick massive layer thought to represent a single flow unit (Branney and Kokelaar, 2002) on the basis of a widespread absence of internal remnant ashfall or pumice-fall layers, erosional contacts, or reworked horizons or soils (Carrasco-Núñez and Branney, 2005). At most sites the ignimbrite shows normal and reverse compositional zoning (Fig. 4), defined by vertical changes in the relative abundance of rhyodacitic (69–71 wt% SiO<sub>2</sub>) and andesitic (54–63 wt% SiO<sub>2</sub>) pumice lapilli: lower parts are dominated by rhyodacite (Fig. 5), and pass gradationally up into a central part with both andesitic and rhyodacite pumice, and this passes gradationally up into a rhyodacitic uppermost part, with no andesitic pumice. The ignimbrite also shows vertical elutriation pipes, well-developed proximal lithic breccias in its central part, and marked concentrations of large (rhyodacitic) pumice cobbles in its uppermost part.

The Zaragoza Member is thought to record a largely sustained explosive eruption that began with a rhyodacitic plinian phase and soon changed to pyroclastic fountaining that generated a large, sustained, radial pyroclastic density current. The composition of the density current was initially rhyodacitic and changed to andesitic as the eruption waxed toward the eruptive climax. At this point, the Los Potreros caldera subsided and large lithic blocks were introduced into the density current. The radial current then gradually reverted to rhyodacitic as the eruption waned, and as the pumice-rich distal limit of the current gradually retreated sourceward it left the discontinuous upper pumice (rhyodacitic) concentration zone. After the current ceased, pumice fallout continued from the extant plinian eruption column (upper rhyodacitic pumice fall layer) until the end of the eruption. New work suggests that the Los Potreros caldera subsided in two stages, initially controlled by a semicircular set of faults along the eastern Los Potreros caldera margin, and then followed by a second, discrete phase of subsidence controlled by a set of extensional faults in the center of Los Potreros caldera: this is recorded by two separate lithic zones within the central part of the Zaragoza ignimbrite at some proximal locations (Willcox, 2011). The Zaragoza magma chamber comprises distinct rhyodacite and andesitic components, possibly as spatially sepa-

rated melt lenses within a partly crystallized subvolcanic pluton (Carrasco-Núñez et al., 2012). It is thought that the lighter, rhyodacite magma resided at higher levels and the denser, less viscous andesitic magma resided at deeper levels. The eruption may have been initiated by intrusion of more mafic magma into the more evolved magma, and it seems that the lower andesitic magma was tapped by the eruption only at times of peak mass flux, when the depth of draw-up was at a maximum. In contrast, at the opening and closing stages of the eruption, the eruptive flux was lower such that the draw-up depth was limited, and only the uppermost rhyodacitic magma was tapped (see models of Blake and Ivey, 1988).

The main ignimbrite flow unit of the Zaragoza ignimbrite is commonly ~15–20 m thick, but it varies from 60 m to less than 2 m in thickness. It shows various lateral variations, due to interaction with local topography. However, it is interesting to note that even where the deposit is less than 2 m thick, it preserves the same double compositional zonation (central lithic-rich zone and upper pumice-concentration zone). This indicates that this thin (<2 m thick) ignimbrite layer must have progressively aggraded during exactly the same time frame as the thicker layer of ignimbrite elsewhere, but up to eight times more slowly (Carrasco-Núñez and Branney, 2005).

The double-zoned Zaragoza ignimbrite shows how vertical variations in lithofacies and composition in an ignimbrite sheet can be used to record temporal changes in nature of the pyroclastic density current (e.g., Branney and Kokelaar, 1997). This is arguably the best way to reconstruct the rapidly changing events during catastrophic caldera-forming explosive eruptions (Branney and Kokelaar, 2002).

### Cerro Pizarro Rhyolitic Dome

#### Definition

Cerro Pizarro rhyolitic dome is a relatively small (~1.1 km<sup>3</sup>), isolated volcano that shows aspects of polygenetic volcanism. These include long-term repose periods (~50–80 k.y.) between eruptions, chemical variations over time, and a complex evolution of alternating explosive and effusive eruptions, including a cryptodome phase, a sector-collapse event and prolonged erosional processes.

Aerial photographs and geologic mapping of Cerro Pizarro reveal an ~2-km-wide, ~700-m-high edifice. The cone is morphologically distinctive (Fig. 6): the central, conically shaped high area is surrounded by a resistant ring with a low, broad apron surrounding the dome. The edifice is open to the west (Fig. 6) and moderately to deeply incised elsewhere by canyons. Geochemical analysis of dome rocks indicates that the majority of erupted material contains 74%–75% SiO<sub>2</sub>, but with different trace-element concentrations (Carrasco-Núñez and Riggs, 2008). The rhyolite is weakly porphyritic, with less than 1% macroscopic sanidine, plagioclase, and quartz as much as 1.5 mm in diameter, and biotite generally no larger than 0.5 mm. The groundmass is variably glassy, with as much as ~25% microphenocrysts of feldspar

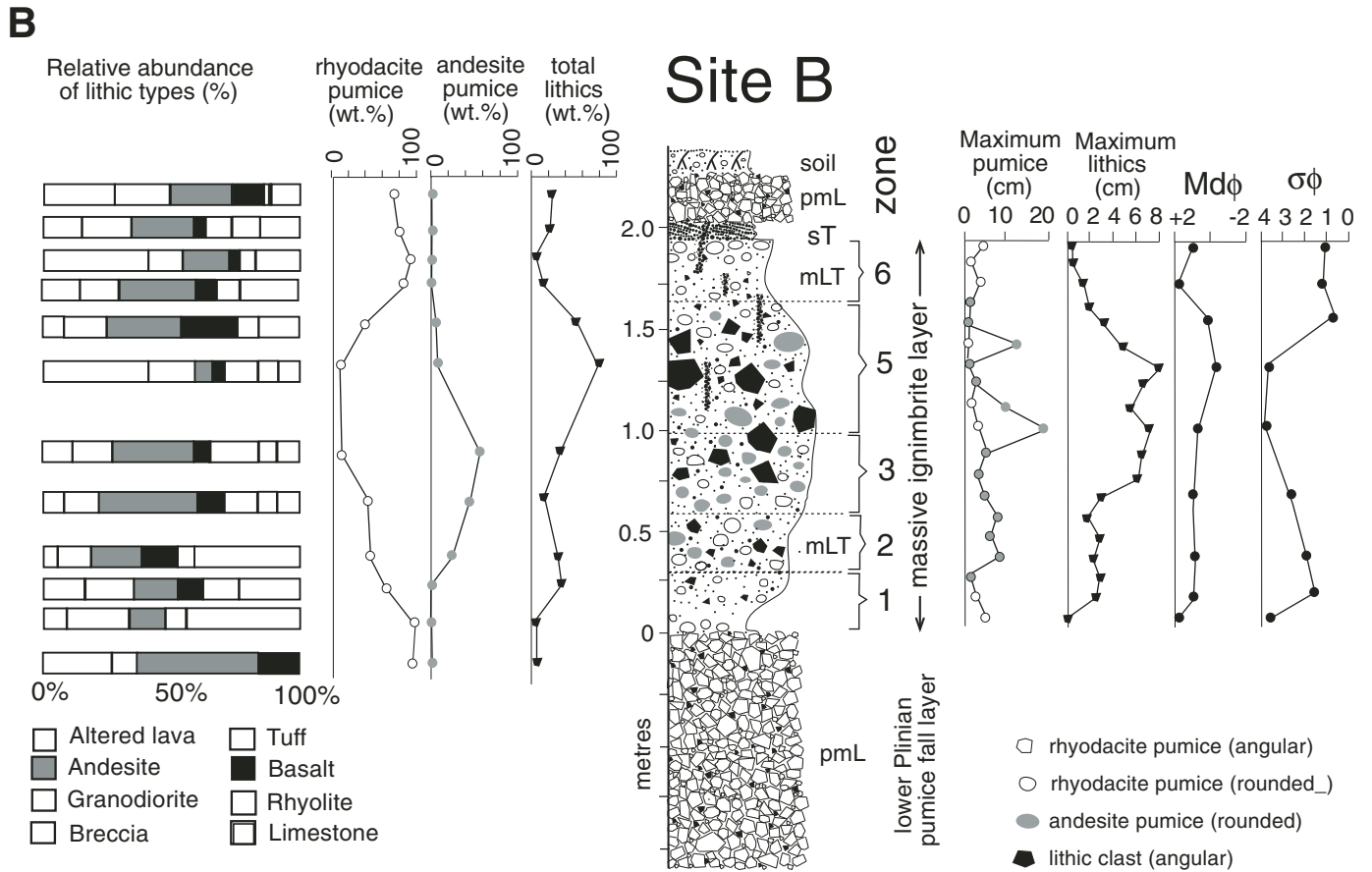
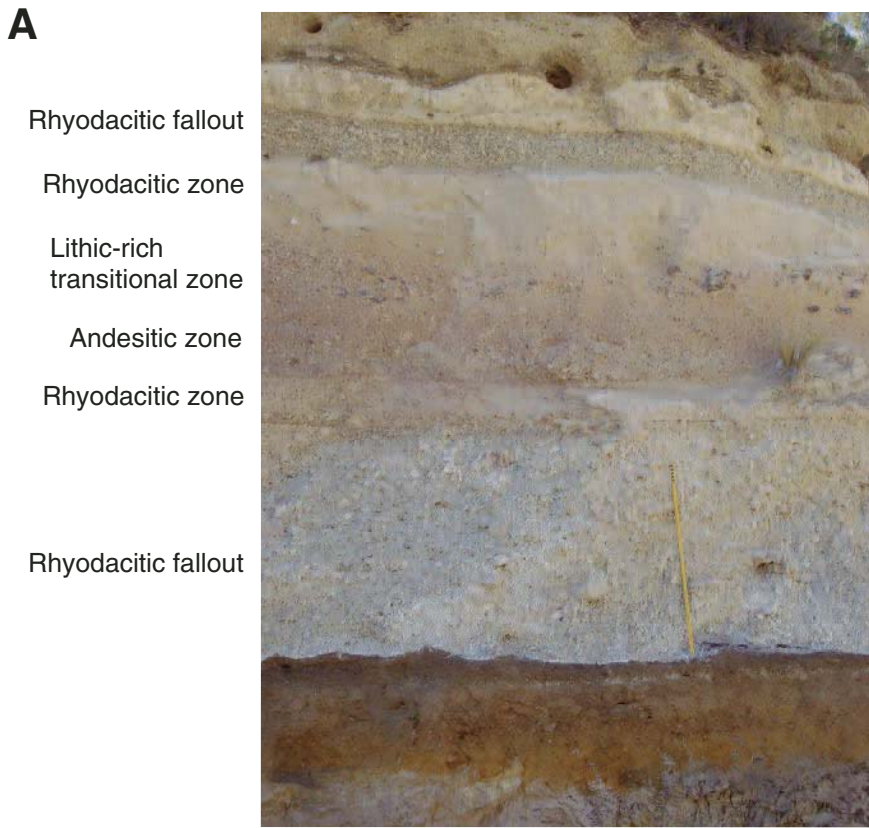


Figure 4. Condensed type section (site B in Fig. 3C) of the Zaragoza ignimbrite showing the different zones of the intraplinian ignimbrite bounded by fall deposits (ruler for scale). Log shows the six zones described by Carrasco-Núñez and Branney (2005) with variations in componentry, proportions of pumice types, and granulometric parameters.

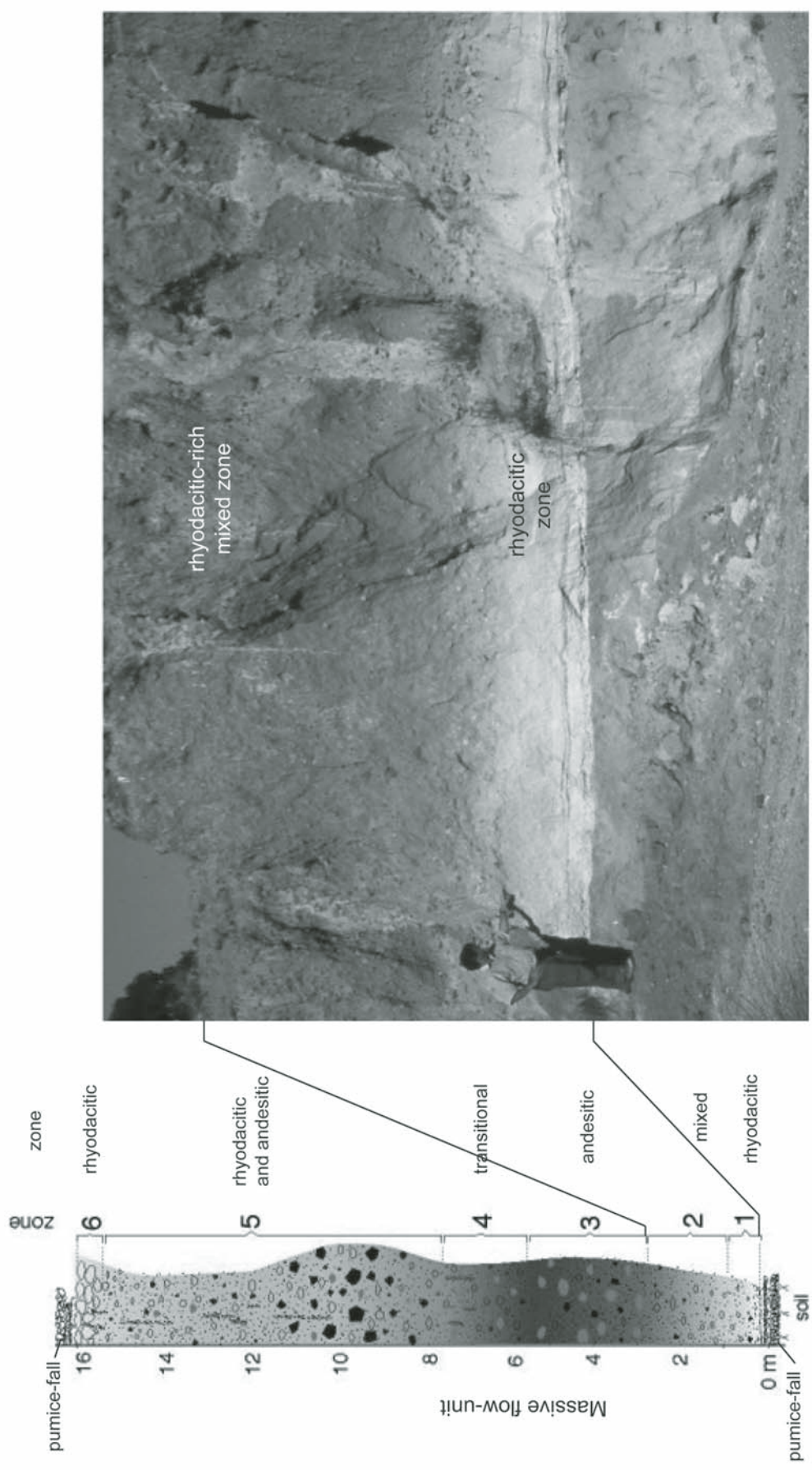


Figure 5. Type section of the Zaragoza ignimbrite, showing the lower zones of the massive flow unit (Stop 7) (Carrasco-Núñez and Branney, 2005).

and biotite. Cerro Pizarro dome comprises two major facies associations, the massive lava dome and the volcanoclastic apron.

### Evolution

The general evolution of Cerro Pizarro took place in four main stages (Riggs and Carrasco-Núñez, 2004; Fig. 7). In the first stage, vent-clearing explosions incorporated xenoliths of basement rocks including vesicular basalts from a nearby scoria cone, Cretaceous limestone, and Xáltipan ignimbrite. Subsequent eruptions produced surge and fallout layers followed by passive, effusive dome growth. Oversteepened flanks of the dome collapsed at times to produce block-and-ash flows, and vitrophyric carapace developed. Blocky pyroclasts, high lithic content, high-density pumice clasts, and occasional bomb sags provide evidence of phreatomagmatism during parts of this stage (McConnell, 2004).

During the second stage, a new pulse of magma caused the emplacement of a cryptodome, which inflated the volcano and strongly deformed the vitrophyric carapace and interior parts of the dome, producing subvertical orientations of the overlying pre-cryptodome units. Disintegration of this cryptodome caused a debris avalanche as the western flank of the volcano collapsed.

The third stage (Fig. 7) was characterized by a prolonged period of erosion of the dome and passive magma intrusion. Erosion cut canyons as much as 30 m deep and produced heterolithic debris- and hyperconcentrated-flow deposits by reworking the debris-avalanche deposited during Stage II. Evidence from iso-

topic dating (Carrasco-Núñez and Riggs, 2008) suggests that the dome quickly regrew into the collapse crater at ca. 116 ka (see below), when the magma filled the crater and formed the present-day conical shape of the volcano. This hypothesis contrasts with the previous interpretation (Riggs and Carrasco-Núñez, 2004), that this dome growth stage was a final eruptive episode after a much longer hiatus. No evidence exists for pyroclastic or collapse-related deposits associated with this dome growth.

After the emplacement of the volcanoclastic deposits formed during Stage III, regional volcanic activity became intense and several pyroclastic successions were produced, including the ca. 100 ka Zaragoza ignimbrite from Los Humeros caldera (Carrasco-Núñez and Branney, 2005), which comprises a basal fallout layer and a massive ignimbrite unit. Two km west of Cerro Pizarro, the fallout and ignimbrite layers overlie the volcanoclastic deposits derived from the sector collapse of Cerro Pizarro (units 2 and 1 in Figure 8A, respectively), and are overlain by fourth-stage pyroclastic deposits of Cerro Pizarro. These pyroclastic deposits together with the reworked deposits associated with the debris avalanche confirm a prolonged hiatus occurred before the volcanic reawakening of Cerro Pizarro.

The fourth and final stage (Fig. 7B) includes both a second hiatus following Stage III dome growth and the final eruptions of Cerro Pizarro, which correspond to renewed activity in the form of explosive eruptions that produced a radially distributed sequence of alternated surge and fall deposits. Low pumice-clast

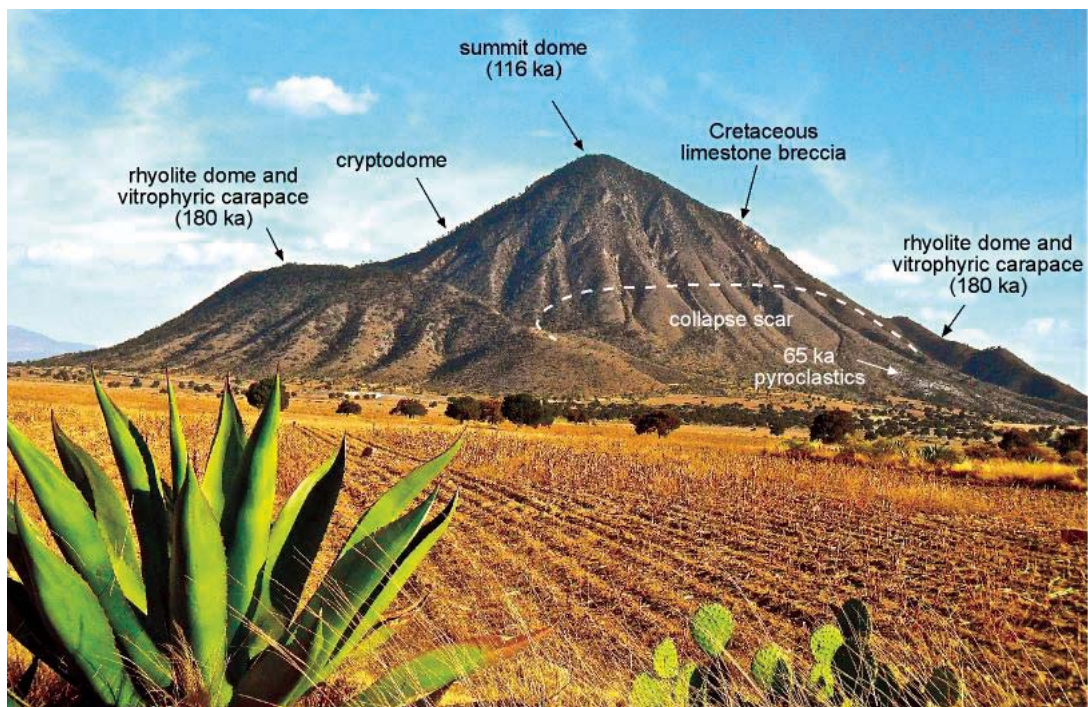


Figure 6. Panoramic view from the west of Cerro Pizarro rhyolitic dome, showing the different components that are indicative of a polygenetic and complex evolution. View from Stop 7.1.

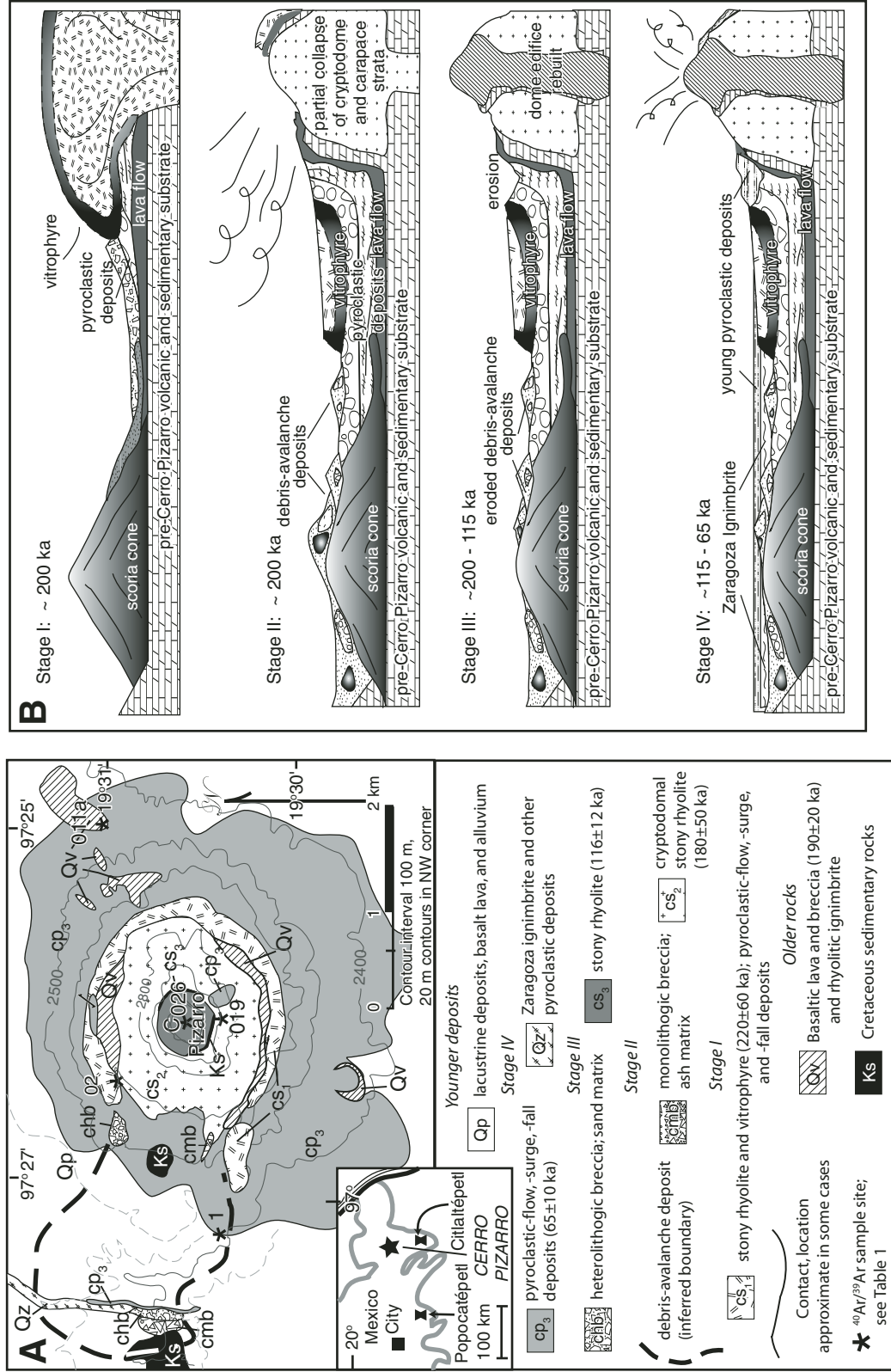


Figure 7. (A) Geologic map of Cerro Pizarro. (B) Evolutionary stages for Cerro Pizarro dome (Riggs and Carrasco-Núñez, 2004).

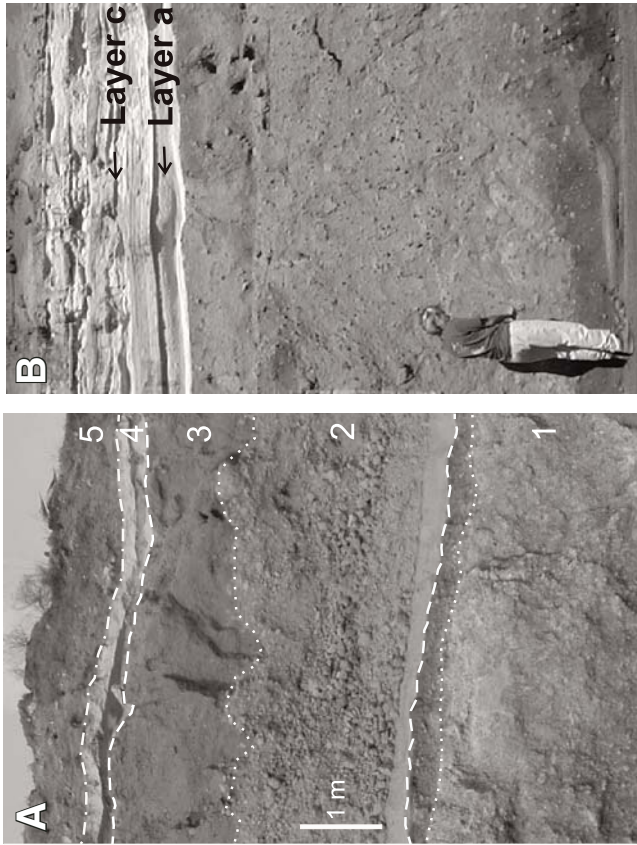
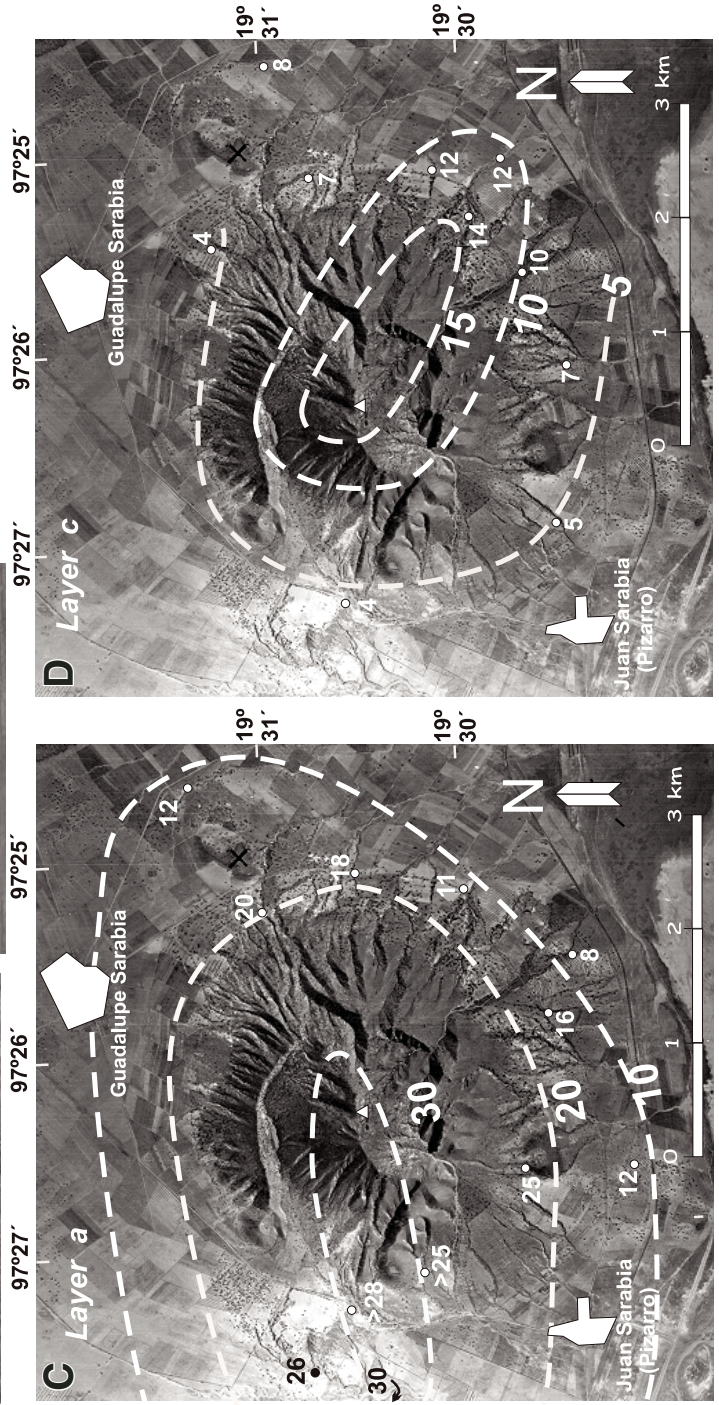


Figure 8. Stratigraphic relations of Cerro Pizarro's units. (A) Photograph showing: 1—debris avalanche deposit derived from C. Pizarro; 2—Zaragoza ignimbrite from Los Humeros caldera; 3—pyroclastic deposits from unknown source; 4—surge and fall deposits dated at 65 k.y. from C. Pizarro. (B) Fall layers (a and c) from C. Pizarro overlying the Zaragoza ignimbrite. (C) Isopach map for layer a. (D) Isopach map for layer c.



densities, together with generally low lithic contents and uniform planar bedding, indicate that these eruptions were dominantly magmatic (McConnell, 2004). The sequence includes two distinctive marker beds: a lower, pumice-rich bed (“a”) that clearly contrasts with the upper, lithic-rich bed (“c”), both of which are widely dispersed around the volcano (Fig. 8B). Riggs and Carrasco-Núñez (2004) first proposed that this locally distinctive white pyroclastic sequence belongs to the Cerro Pizarro activity based on its apparent distribution around the volcano, and rhyolitic composition similar to that of the Cerro Pizarro rocks; this hypothesis was reinforced by Carrasco-Núñez and Riggs (2008), who presented isopach maps (Fig. 8C and 8D) that more precisely demonstrate the radial nature of these deposits and their likely source at Cerro Pizarro. These units are critically important as they are the main evidence of a long life span of Cerro Pizarro, as demonstrated by isotopic dating of samples taken from layer “a,” dated at 65 ka (Carrasco-Núñez and Riggs, 2008).

### **Interpretation**

Cerro Pizarro rhyolitic dome evolved through periods of effusive and highly explosive activity that were separated by cryptodome intrusion, edifice sector-collapse, and prolonged erosional episodes (Riggs and Carrasco-Núñez, 2004). Chemistry of the eruptive products also changed over time. This complex evolution, in addition to the ca. 50–80 ka repose period between the main eruptive episodes, indicates that a model of short-lived, monogenetic activity does not characterize all rhyolite domes. This eruptive behavior provides new insights into how rhyolite domes evolve. A protracted, complex evolution bears important implications for hazard assessment if reactivation of an apparently extinct rhyolitic dome must be seriously considered.

### **Implications for Hazards Assessment**

Reactivation of a rhyolitic dome after a long period of repose has not been recognized at any other volcano, and carries very important implications for assessment of volcanic hazards, particularly considering that renewed activity might be explosive or involve sector collapse of the volcanic edifice. Regardless of whether a dome like Cerro Pizarro should be considered polygenetic or monogenetic, the combined stratigraphic, geochemical, and geochronologic evidence from the volcano shows that a rhyolite dome has the potential for renewed activity after a long hiatus. We speculate that complex behavior in the Cerro Pizarro system may be a function of its isolation from other domes or volcanoes—other domes in the Serdán-Oriental basin are no farther away from Cerro Pizarro than the distribution of the Inyo domes, for example (i.e., ~10 km), but in every other case we know of, dike-fed domes like the Inyo or South Sister systems occur in a semi-continuous chain rather than as a series of isolated volcanoes. Dome eruptions in the Trans-Mexican Volcanic Belt, or any district where rhyolitic domes seem to erupt in isolation from other, larger systems, will serve as an excellent test to assess the apparent severe hazards associated with these small volcanoes.

## **Cerro Pinto Tuff Ring–Dome Complex**

### **Definition**

Cerro Pinto is a Pleistocene rhyolite tuff ring–dome complex. The complex is composed of four tuff rings and four domes that were emplaced in three eruptive stages marked by changes in vent location and eruptive character.

### **Evolution**

The evolution of Cerro Pinto as proposed by Zimmer (2007) and Zimmer et al. (2010) includes three distinct stages (Fig. 9). During Stage I, vent-clearing eruptions produced a 1.5 km-diameter tuff ring (southern) that was then followed by emplacement of two domes (I and II) of ~0.2 km<sup>3</sup> each. With no apparent hiatus in activity, Stage II activity initiated with the explosive formation of a tuff ring ~2 km in diameter adjacent to and north of the earlier ring. Subsequent Stage II eruptions produced two smaller tuff rings nested within the northern tuff ring as well as a small dome that was mostly destroyed by explosions during its growth. Stage III involved the explosive evacuation of a small crater and the emplacement of a 0.04 km<sup>3</sup> dome within this crater. Similar to Dome II, Dome IV uplifted and deformed previously emplaced tephra deposits.

### **Interpretation**

Cerro Pinto’s eruptive history includes sequences that follow simple rhyolite-dome models, in which a pyroclastic phase is followed immediately by effusive dome emplacement. Some aspects of the eruption, however, such as the explosive reactivation of the system and explosive dome destruction, are rarely documented in ancient examples. These events are commonly associated with polygenetic structures, such as stratovolcanoes or calderas, in which multiple pulses of magma initiate reactivation. A comparison of major and trace element geochemistry with nearby Pleistocene silicic centers does not show indication of any co-genetic relationship, suggesting that Cerro Pinto was produced by a small, isolated magma chamber. The compositional variation of the erupted material at Cerro Pinto is minimal, suggesting that there were not multiple pulses of magma responsible for the complex behavior of the volcano and that the volcanic system was formed in a short time period.

The variety of eruptive styles observed at Cerro Pinto reflects the influence of quickly exhaustible water sources on a short-lived eruption. The rising magma encountered small amounts of groundwater that initiated explosive eruptive phases. Once a critical magma/water ratio was exceeded, the eruptions became dry and sub-plinian. The primary characteristic of Cerro Pinto is the predominance of fall deposits, suggesting that the level at which rising magma encountered water was deep enough to allow substantial fragmentation after the water source was exhausted. Isolated rhyolite domes are rare and are not currently viewed as prominent volcanic hazards, but the evolution of Cerro Pinto demonstrates that individual domes may have complex

cycles, and such complexity must be taken into account when making risk assessments.

### Atexcac Maar (Axalapaxco)

#### Definition

Atexcac is a maar volcano excavated into pyroclastic deposits, basaltic lava flows (Fig. 10C) and the flanks of a scoria-cone cluster (Fig. 10D), which itself was built on a limestone topographic high (Fig. 10). The crater, and the enclosed lake (Figs. 10B and 10C), have an elliptical shape with a diameter from 1150 to 850 m. Atexcac is ~120 m deep; the water depth is ~40 m (of the total 160 m), and ~60 m is below the pre-eruptive ground

surface. It is elongated to the ENE with beds, mostly unconsolidated, that dip outward at 16–22°.

#### Evolution

The evolution of the Atexcac crater was first interpreted by Romero (2000) and later refined by Carrasco-Núñez et al. (2007). At least four different units were proposed for the maar sequence (Fig. 10A). Initial short-lived phreatic explosions started at the southwest part of the crater and were followed by an ephemeral open-vent vertical column. The influx of external water led to shallow explosive interactions with the ascending basaltic magma and produced a sequence of surge-dominated deposits with numerous cross-bedded layers, bomb sags, channels, a few

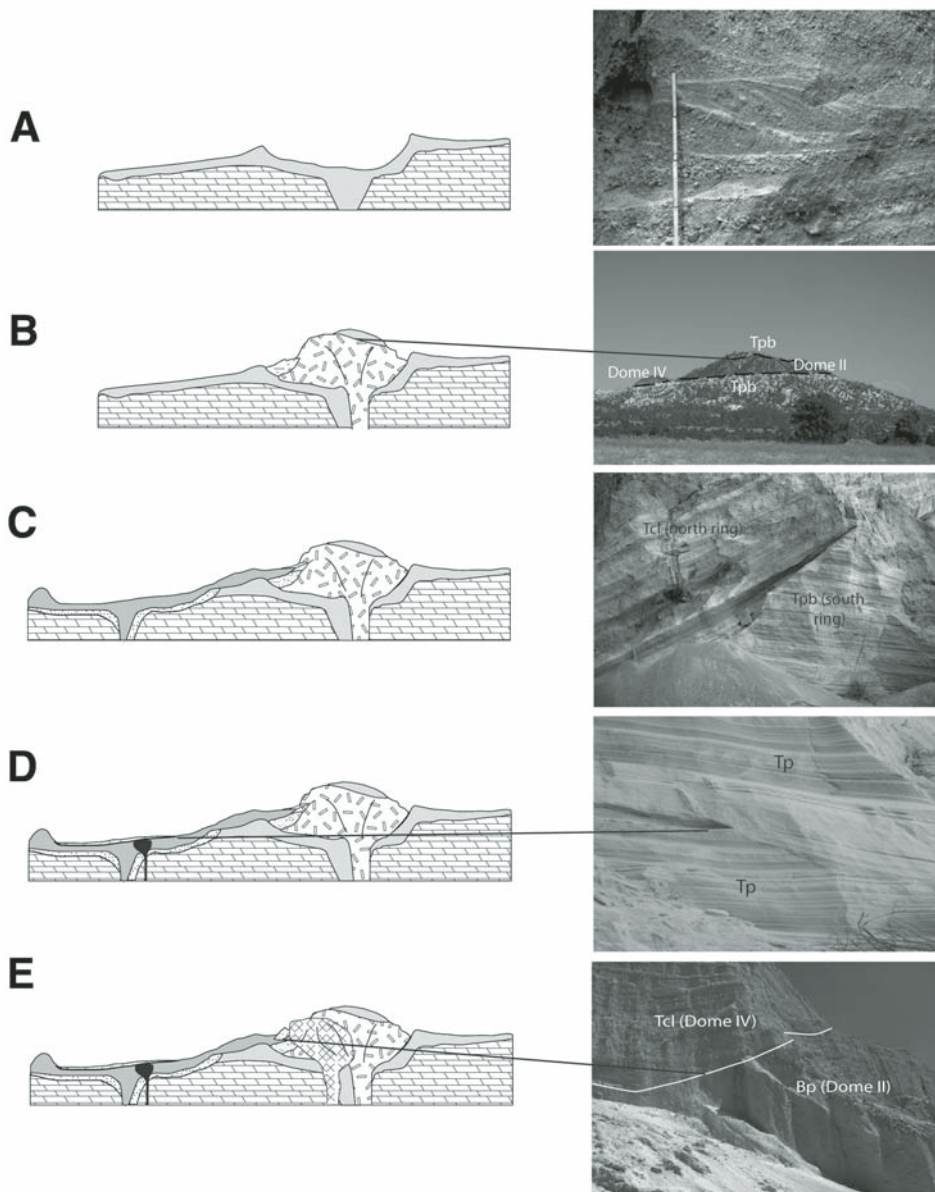


Figure 9. Evolution of Cerro Pinto tuff ring-dome complex (Zimmer et al., 2010). (A) Stage I excavation of South ring; photo shows cross-bedded biotite-rich pumice tephra. (B) Stage I emplacement of Domes I and II. Pyroclastic deposits (Tpb) emplaced during building of the tuff ring uplifted on Dome II. Photo view to east. (C) Stage II eruption of North tuff ring. Photo shows a scoured contact between lithic-rich tephra (Tcl) and facies (Tpb) of the South ring. (D) Excavation of the northern and western inner rings. Deposits of all North ring eruptions are lithic-rich tephra; deposits of different eruptions are distinguished by scoured contacts, as shown in photo. (E) Stage III excavation of a small crater and emplacement of Dome IV. Photo shows lithic-rich tephra within the crater scoured into interbedded grain flow and surge deposits.

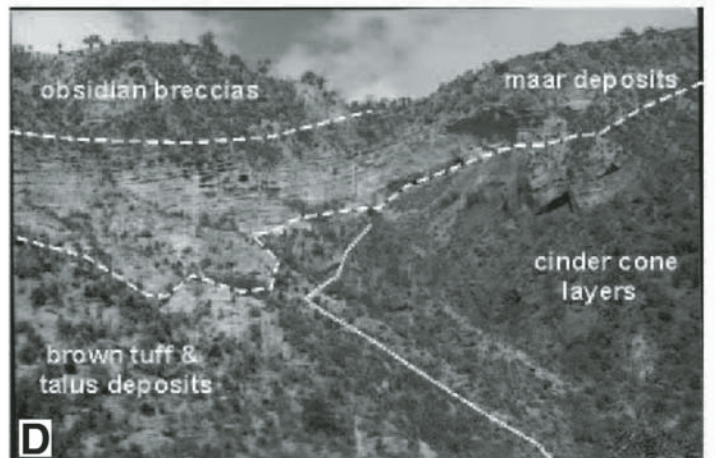
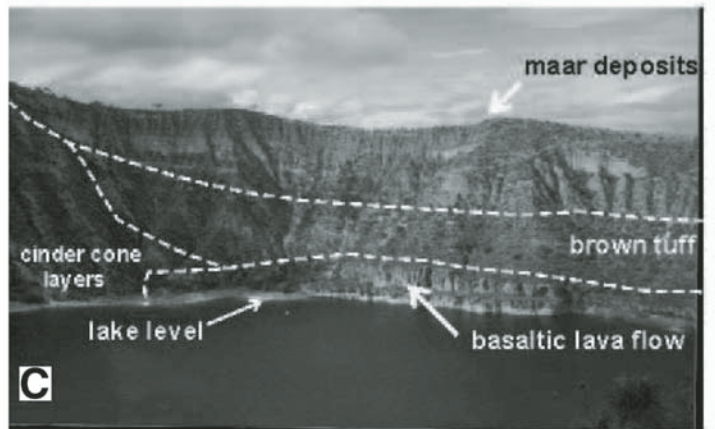
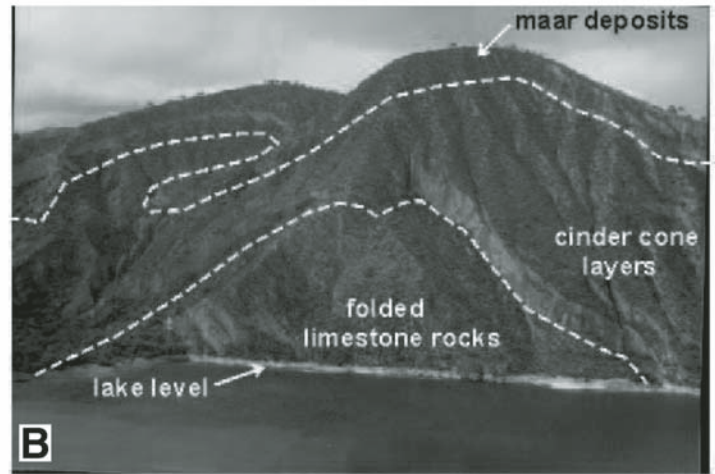
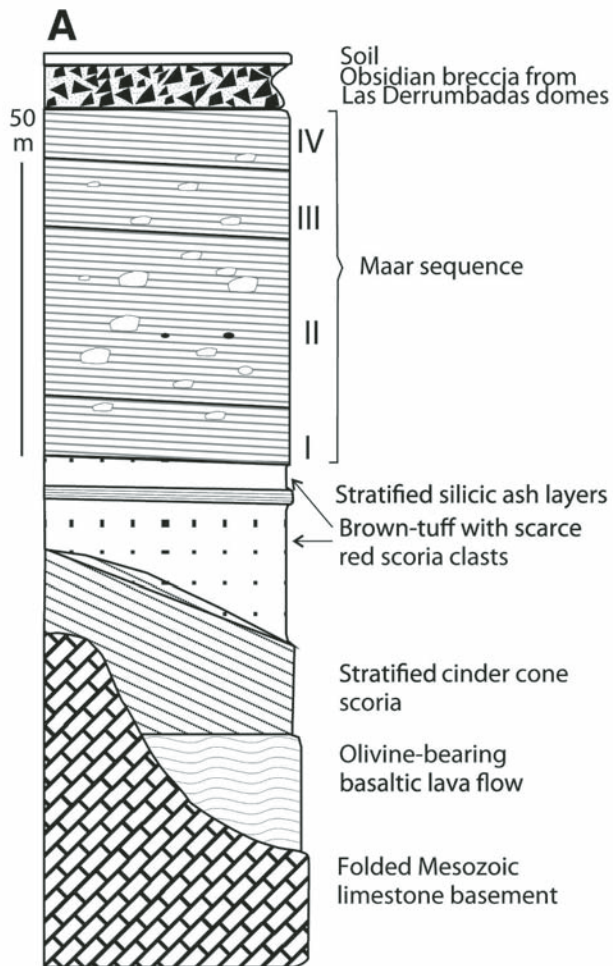


Figure 10. (A) Summary of the stratigraphy of the Atexcac crater and photographs of the crater interior. (B) View to the north showing the relations of country rocks: folded limestone underlies a cinder cone. (C) Basaltic lava flow underlies the maar-forming deposits at the north-eastern wall. (D) Maar-forming deposits underlie an obsidian breccia from Las Derrumbadas domes, and overlie brown tuff and cinder layers.

dune forms and layers with accretionary lapilli. Drier explosions progressed downward and/or laterally northward, sampling sub-surface rock types, particularly intrusive, limestone and andesitic zones; these eruptions were caused by repetitive injection of basaltic magma (Fig. 11). A new migration back to the southwestern area is inferred to occur later, producing abundant small andesitic clasts in the S-SW upper deposits at the time large intrusive and limestone blocks were sampled. This suggests differential degrees of fragmentation due to inherited fragmentation and/or relative distance to the locus of explosions. A final explosive phase involved a new injection of magma and new migration of explosions to or close to the highly fractured andesitic aquifer, causing an influx of external water and wetter conditions at the end of the maar formation.

**Interpretation**

The Atexcac crater was formed by vigorous phreatomagmatic explosions in which fluctuations in the availability of external water, temporal migration of the locus of the explosion, and periodic injection of new magma were important controls on the evolution of the maar crater. Variations in grain sizes and component proportions in correlated deposits from the different sections suggest that a migration of the locus of explosions produced different eruptive conditions and fluctuating water-magma interactions. Deposits rich in large intrusive and limestone blocks are associated with a matrix enriched in small andesitic lapilli. This could suggest differential degrees of fragmentation due to inherited (previously acquired) fragmentation and/or relative distance to the locus of explosions.

Carrasco-Núñez et al. (2007) inferred that the aquifer formed in fractured rocks, predominantly andesitic lava flows and limestone. Andesitic accessory clasts dominate in all stratigraphic levels but these rocks are not exposed nearby. These local hydrogeological conditions contrast with those at nearby maar volcanoes, where the water for the magma/water interactions apparently mostly came from an unconsolidated tuffaceous aquifer, producing tuff rings.

**ITINERARY**

Road logs for this field trip guide are provided here; stops for Days 2 and 3 of this field trip are shown in Figure 12.

**Day 1**

Drive to the field area, and arrival at the Hotel Covadonga in Perote, Ver. Dinner.

**Road Log, Day 1—Querétaro to Field Area (Perote, Veracruz)**

<i>km</i>	<i>Directions</i>
0.0	Meet at the Misión Juriquilla Hotel parking lot.

2.45	Merge onto motorway No. 57 southbound toward Querétaro City.
14.0	Drive through the Querétaro City and continue over motorway 57 southbound to Mexico City.
120.0	Drive for ~100 km and take the junction to Puebla at the Arco Norte motorway.
320.0	Continue on the Arco Norte for over 200 km and take the exit to Apizaco/Huamantla, after the second exit to Calpulalpan.
400.0	Pass through the outskirts of Apizaco and Huamantla on road 136.
430.0	Follow signs to Veracruz/Xalapa and merge onto toll road 140D.
450.0	Pass the tunnel through Cerro Grande Mountains and cross into the Libres-Oriental basin.
460.0	Drive through the Tepeyahualco lava; note Cerro Pizarro toward the east and Los Humeros caldera toward the northwest.
480.0	Take the Perote exit toward the right-hand side (east).
483.0	Drive 3 km southbound toward the town of Perote.
486.0	At the major intersection in town, turn right onto road 140 toward Puebla (SW).
488.0	Drive for 1.1 km until to Hostería Covadonga Hotel on the left side of the road.

**Day 2**

On Day 2 we will examine the deposits of Los Humeros caldera. Stops for Day 2 are shown in Figure 12.

**Road Log Day 2—Perote to Los Humeros Caldera**

<i>km</i>	<i>Directions</i>
0.0	Meet in the morning at the hotel restaurant.
0.3	Take road 140 toward Perote for 300 m and turn left (northbound) onto Reforma street; follow this road for 14.2 km.
14.5	Turn right at dirt track; drive for 2.7 km.
17.2	Turn right at junction for other 500 m.
17.7	Arrive at pumice quarry, <b>Stop 1</b> , to see the Faby Formation at the caldera slope.
20.9	Drive back the same way to merge onto the main road toward the caldera. Drive up the winding road for 5.2 km.
26.1	Stop on the side of the road for a panoramic view of the Serdán-Oriental basin. On a clear day, Cofre de Perote, Citlaltépetl, Cerro Pizarro, and other volcanoes are visible ( <b>Stop 2</b> ).
27.2	Continue on caldera road for 1.1 km and stop at Vigía Alta on the southern caldera rim to

South wall representative column

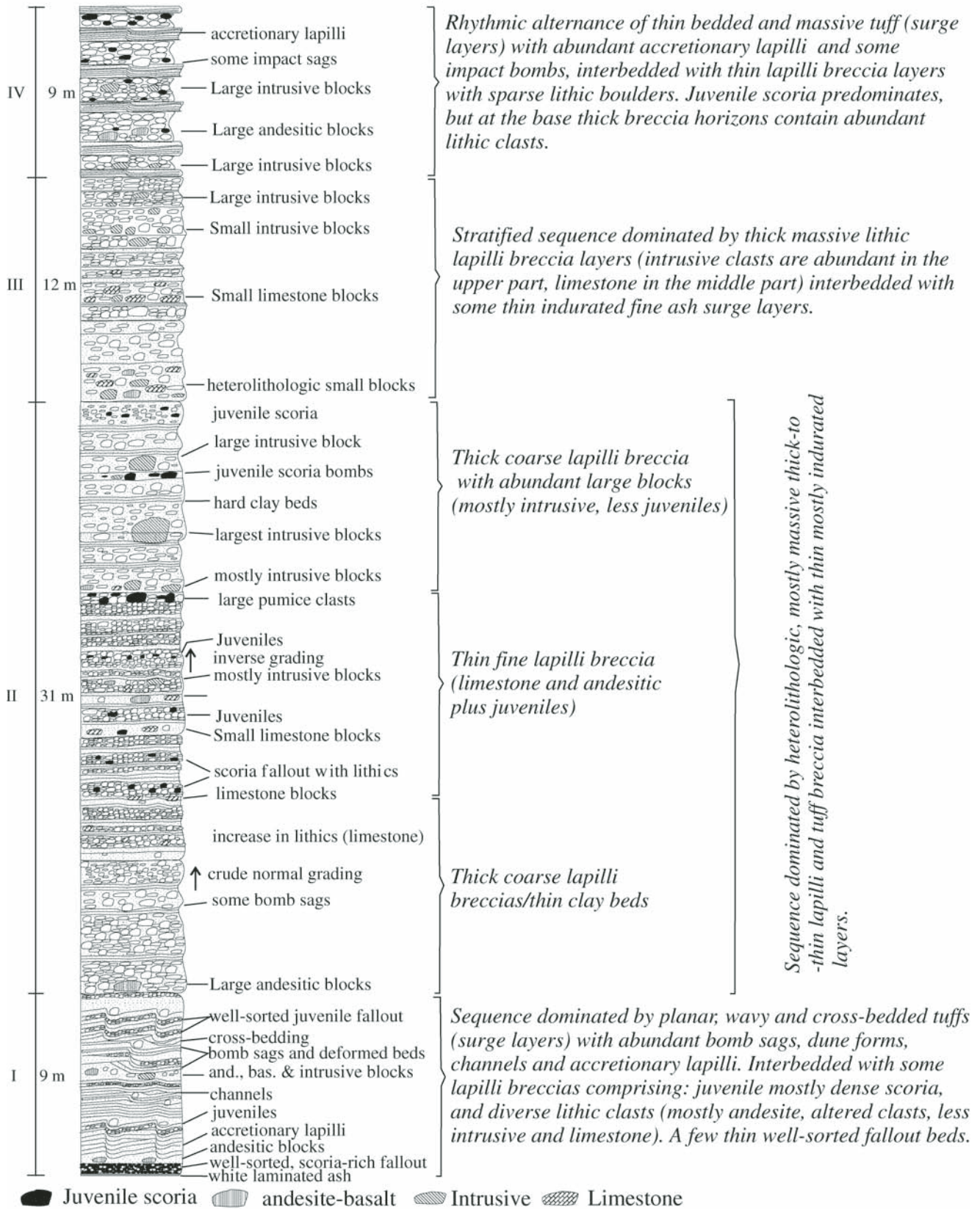


Figure 11. Representative stratigraphic log for the southern wall of Atexcac crater (Carrasco-Núñez et al., 2007).



- see spatter and scoria agglomerates from Holocene eruptions (**Stop 3**).
- 29.1 Keep on main road for 1.9 km, now inside the caldera. Turn right (NE) onto a dirt track. Drive for 1.4 km.
- 30.5 Turn left over a narrow track through a field.
- 31.3 Follow this road for 800 m to the dry *arroyo* (stream).
- 32.0 Drive carefully in the pumiceous gravel arroyo for 700 m and stop by a gully on the right-hand side (east). Park here and walk for 100 m to **Stop 4**. Lunch time.
- 35.0 Drive back the same way toward the main road and turn right (northbound) toward the Comisión Federal de Electricidad (CFE) camp and Maztaloya village.
- 40.2 After 5.2 km on the main road past the first geothermal wells, turn left (west) exactly where the road bends into a dirt track.
- 40.5 Drive down the dirt track for 300 m and park for **Stop 5**, lavas over pyroclastic deposits.
- 40.8 Return to the main road again and drive toward the north.
- 46.6 Pass the Humeros village and turn right into a single track road and we'll see producing geothermal wells, turbines and the producing plants (**Stop 6**).
- 77.0 Return to Perote for dinner.

### Stop 1. Los Frijoles Quarry to See the Faby Pyroclastic Succession

Location: UTM 14Q 671760/2171119

This quarry is the type locality for the Faby Formation, however the Zaragoza ignimbrite (Potreritos Formation), Xoxocitic Member (Rosa Formation) and thin vestiges of the Cuicuiltic Member are also exposed. This locality exposes four soil-bounded Plinian pumice-fall deposits of the Faby Formation (Fig. 13). In ascending order these are:

1. The  $230 \pm 40$  ka,  $>2.39$  km<sup>3</sup> (DRE) rhyolitic Perote Member (this eruption unit has three subdivisions, which are not easily distinguished at this locality).
2. The  $260 \pm 40$  ka  $>1.77$  km<sup>3</sup> (DRE) andesitic-rhyolitic Frijol Member (this eruption unit has five subdivisions, but notice the lack of internal paleosols; elsewhere the Frijol Member is locally overlain by fluvio-deltaic sediments, suggesting a more extensive post-deposition hiatus).
3. The  $140 \pm 20$  ka  $>1.68$  km<sup>3</sup> (DRE) dacitic Aguila Member.
4. The ca. 140 ka andesitic-dacitic Zorrillo Member. This eruption unit contains a range of different pumice types, including mingled pumice, and is interpreted as recording significant magma chamber heterogeneity and pre-/syn-eruption mingling. The Zorrillo and underlying Aguila Members are thought to record precursory eruptions

to the caldera-forming Zaragoza eruption because the timing of their eruption is within error of the Zaragoza eruption ( $140 \pm 12$  ka; Willcox, 2011).

Isopach and isopleth maps have been constructed for the Plinian deposits, but data points are insufficient to locate the vent positions within the caldera with accuracy. Exceptions to this are the upper divisions F4–F5 of the Frijol Member, which appear to have vented along the southern inferred rim of Los Humeros caldera (Willcox, 2011). Paleosols developed on each eruption unit indicate hiatuses at these southern-rim localities. Other eruptions, however, were probably occurring during this time as indicated by (a) two successions of Faby Formation age outside of the western and northwestern margins of Los Humeros caldera that are not present in the intra-caldera Faby plinian stratigraphy, and (b) the occurrence of andesitic scoria in Division F1 of the Frijol Member and as lenses within the palaeosols on the Aguila and Zorrillo members: these scoria deposits record minor background mafic volcanism, probably mainly restricted to within the margins of Los Humeros caldera (the deposits of which are now presumably deeply buried; Willcox, 2011). Between the Zorrillo Member and overlying Zaragoza Member (basal fall deposit and ignimbrite) is a compound (double) paleosol. At a nearby locality this paleosol bifurcates, revealing intervening thin beds of pumice and scoria lapilli and ash. Eruption frequency estimates for the Faby Formation (pre-Los Potreritos caldera subsidence) and for post-Los Potreritos caldera subsidence (Willcox, 2011) suggest that the frequency of eruptions was actually greater before subsidence of Los Potreritos caldera (Ferriz and Mahood, 1984).

### Stop 2. Panoramic View of the Serdán-Oriental Basin–Cofre de Perote-Citlaltépetl

Location: UTM 14Q 669411/2170585

View of the Serdán-Oriental volcanism, and the Citlaltépetl–Cofre de Perote volcanic chain. The northernmost volcano of the chain is the shield-like Cofre de Perote andesitic-dacitic compound volcano. Its last activity occurred ca. 200 ka, but repeated sector-collapse events have occurred long after the cessation of its eruptive activity producing debris-flow and avalanche deposits at ca. 40 ka and 13 ka with runout distances of ~65 and 30 km downstream, respectively (Carrasco-Núñez et al., 2010). However, the summit scarps affect the eastern flank of the volcanoes, and they are not visible from this view. The volcanic chain also includes La Gloria and Las Cumbres volcanic complexes and the active Citlaltépetl andesitic stratovolcano. The extinct Sierra Negra andesitic stratovolcano is the southernmost edifice of this chain.

A panoramic view of the Serdán-Oriental basin allows us to compare the morphology of the different volcanic edifices, with the Cerro Pizarro polygenetic dome, in the foreground, the asymmetric profile of the Alchichica tuff ring inclined to the east, the prominent relief of the Las Derrumbadas twin rhyolitic domes; and behind Cerro Pizarro and to the west of Las

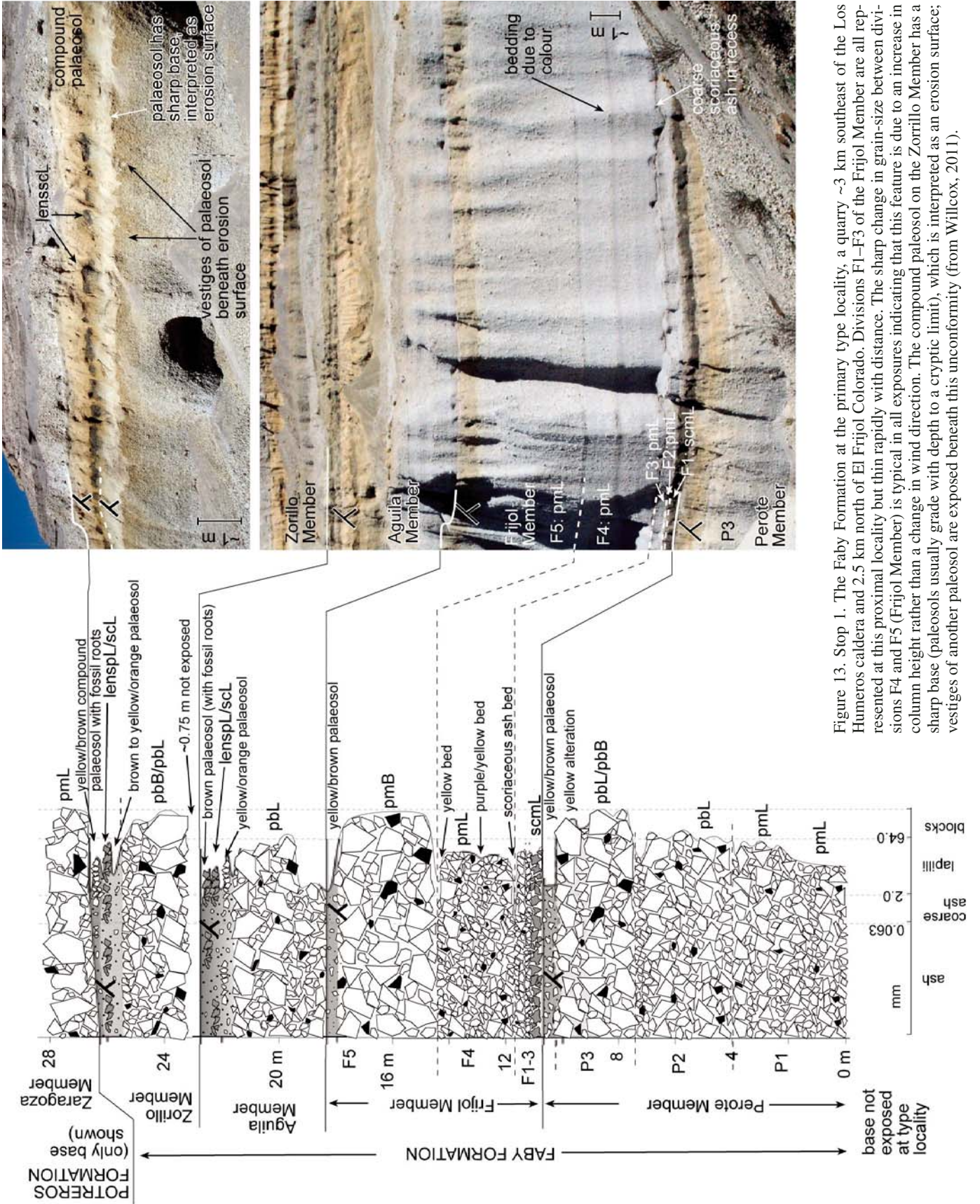


Figure 13. Stop 1. The Faby Formation at the primary type locality, a quarry ~3 km southeast of the Los Humeros caldera and 2.5 km north of El Frijol Colorado. Divisions F1–F3 of the Frijol Member are all represented at this proximal locality but thin rapidly with distance. The sharp change in grain-size between divisions F4 and F5 (Frijol Member) is typical in all exposures indicating that this feature is due to an increase in column height rather than a change in wind direction. The compound palaeosol on the Zorillo Member has a sharp base (palaeosols usually grade with depth to a cryptic limit), which is interpreted as an erosion surface; vestiges of another palaeosol are exposed beneath this unconformity (from Willcox, 2011).

Derrumbadas, the irregular profile represents the Cerro Pinto tuff ring–dome complex.

### Stop 3. Caldera Rim Volcanism—Strombolian Spatter Agglomerate and Proximal Scoria Fall Deposits

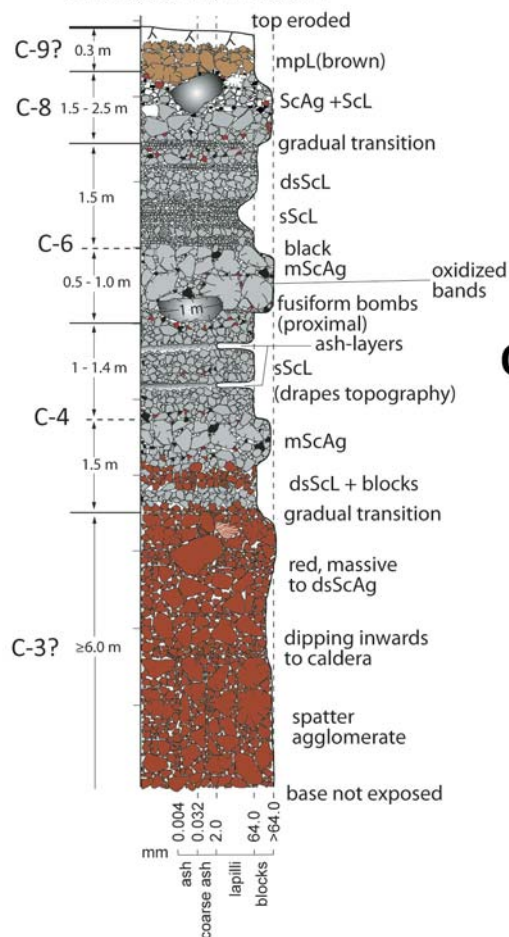
Location: UTM 14Q 668945/2170804

We will drive up the winding road that leads into the Los Humeros caldera and stop at the outer caldera rim at an area locally named Vigía Alta. At this locality we can see the products of some of the most recent eruptions of Los Humeros caldera (Fig. 14). The base of the succession is not exposed here but its position can be inferred from nearby exposures of stratigraphically lower units. The succession here starts with red, oxidized spatter agglomerates up to 6 m thick that were likely erupted from a nearby vent. Agglomerate is covered directly by

a coarser and less homogeneous, mainly black layer 5 m thick that forms a crudely stratified scoria lapilli layer with alternations of large juvenile blocks ( $\leq 1.5$  m in diameter). Impact structures and bomb sags are evident at this locality. This is followed by diffusely stratified scoria lapilli that grades into coarser clasts of similar composition with crude inverse grading. Accidental lithic clasts are scattered among most of the basaltic succession, composed mainly of older andesite lavas and other altered volcanic rocks. The top of the exposure is a more lithic-rich, brown layer of coarse lapilli and blocks of very irregular shapes that passes up into a paleosol. Most of the succession dips inward toward the caldera center.

These basaltic to basaltic-andesite layers are proximal Strombolian scoria-fall deposits intercalated with larger blocks and ballistic bombs resulting from energetic pulses from one or more vents. The succession correlates with the basaltic/andesite

#### A Roadside Vigía Alta southern rim UTM: 668945 / 2170804



#### B



#### C



Figure 14. Stop 3: Products of basaltic caldera-rim volcanism at Vigía Alta, southern rim of Humeros caldera. (A) Graphic log of the succession exposed at the road cut showing red, oxidized spatter agglomerate overlain by massive to stratified scoria lapilli beds with bomb-rich layers. (B) Panoramic view of the exposure showing mainly layers C4 and C6. Note person for scale. (C) Close-up photo of layers C4 and C6 showing highly angular proximal bombs bracketed by massive to diffusely stratified scoria lapilli.

part of the layered Cuicuiltic Member, mainly layers C4, C6, and C8. Numerous scoria cones are exposed along most of the southeast margin of the caldera; most of these structures probably record small fissure eruptions that took place between stages of more explosive volcanism within the caldera. The morphology of such small volcanoes (~15 craters) varies widely, consistent with the broad spectrum of ages. Some may be older than 50 ka, but the most recent ones are younger than 10,000–5000 years old.

#### **Stop 4. Los Potreros Stratigraphy and Cuicuiltic Member Type Section**

Location: UTM 14Q 666756/2173722

From Stop 3, drive 1.9 km, turn right onto a dirt road to Altolucero village. At 1.4 km turn left down the valley and through a wadi for 800 m. Exposures of pumiceous material indicate the interior of the nested Potreros caldera; the caldera scarp runs nearly N-S inside the larger Los Humeros caldera. Gullies incised into the western slope of the scarp reveal the pyroclastic stratigraphy down to the Zaragoza ignimbrite, which is associated with subsidence of Los Potreros caldera. Walk for 100 m up the gully to exposures of the post-Zaragoza eruptive succession.

The succession starts with hydrothermally altered lithic breccias, probably part of the Zaragoza ignimbrite, overlain by a stratified to massive layer of scoria lapilli. This scoria layer grades into a paleosol that is overlain in turn by the ~5-m-thick Xoxoctic pumice-fall layer, which exhibits a stratified lithic-rich base with intercalated layers of ash. At other locations, where the ash layers are thicker, accretionary lapilli are locally preserved. A thick, diffuse-stratified layer of pumice lapilli, with clasts from 1 to 30 cm in diameter, overlies the Xoxoctic pumice-fall layer and a well-developed paleosol. This pumice lapilli layer is overlain by a brown ignimbrite, locally named the Llano ignimbrite (Willcox, 2011), that consists of lithic-rich lapilli tuff with lenses of dense pumice and cross-lamination. Patches of reworked material occur at some levels. The Llano ignimbrite reaches 4 m in thickness, and exhibits subtle normal grading.

Most of the contrasting layers of the Cuicuiltic Member are exposed at this locality, with well-established thicknesses and componentry characteristics. The Cuicuiltic Member forms a well-defined eruption unit that has a well-developed paleosol at the base and grades upwards into the present-day soil, often with an eroded top. It has been subdivided into nine layers that each extend for more than 8 km<sup>2</sup>. These layers have been named C1 to C9 from base to top respectively (Fig. 15). C1 is a lithic-rich pumice lapilli layer with a thin soil-rich layer at the top. This is overlain by C2, the thickest and most extensive of the Plinian pumice layers, which reaches 6 m thick at proximal localities. C2 is composed of coarse- to medium-grained pumice lapilli, stratified and with a thin ash layer at the middle levels. C3 is characterized by the presence of mingled and mixed rhyodacite and andesitic pumice. C4 is a fine-grained black sandy layer, overlain by coarse, clast-supported massive scoria lapilli with a stratified top. Overlying the black andesitic lapilli is C5, with a thin 5–20-cm-

thick layer of pale gray pumice with shiny red lithic clasts. C6 is a 1.2-m-thick layer of massive to stratified, faceted scoriaceous lapilli. It is followed by C7, a layer with abundant clasts of mingled pumice and a mixture of andesitic and rhyodacitic pumice with a slightly bedded top. The top layers are C8 and C9. C8 is a coarse-grained pumice lapilli and blocks layer that is crudely stratified and with interbedded diffuse white pumice layers. It commonly contains impact sags from scoria bombs. The top is commonly eroded and is locally represented by C9, a 1.5-m-thick lapilli layer that is diffusely stratified. Pumice clasts are gray with some mingling textures. C9 grades up into a paleosol.

The Cuicuiltic Member represents the last explosive eruption at Los Humeros caldera. The eruptive sequence started with Plinian explosions that ejected rhyodacite pumice followed by a short hiatus. C2 records a more voluminous eruption that deposited thick pumice-fall layers. Eruption of C3 was triggered by injection of a more basic (basaltic-andesite) intrusion into the volcano, as suggested by the presence of mingled pumice that may have sampled other, more basic parts of the magma chamber. The rhyodacite eruption probably ceased while lateral contemporaneous vents of basaltic to andesitic composition began to erupt scoriaceous lapillus that formed C4. No andesitic material is present in C5, suggesting a pause in mafic fissure eruptions. C5 records yet another reactivation of the silicic vent with the deposition of 4 m of silicic pumice near the source vent. Fissure vents to the north of the caldera were then re-activated and again ejected scoriaceous material as recorded by layer C6, possibly including discrete explosions that formed pumiceous density currents. By C7, an efficient mixture had taken place and mixed and mingled pumice were erupted from the main vent, forming massive pumice layers. C8 is disrupted by deposits of an explosive Strombolian eruption near Maztaloya village while white pumice lapilli continued to fall from the umbrella cloud. The eruption ended with C9, a well-mixed, diffusely stratified andesitic lapilli.

#### **Stop 5. Lava Overlying Young Pyroclastics: El Pájaro Holocene Lava and the Cuicuiltic Member**

Location: UTM 14Q 662579/2172822

Return to the main road toward the northwest. Past the CFE camp and the village of Maztaloya, turn left into a dirt track to the southwest for 300 m. This exposure is 200 m NW of the Xalapasco crater.

The exposure reveals the front lobe of a large lava field, known as the El Pájaro lavas because of the bird-like shape of the lava from a satellite or digital elevation model image. The lava field is probably Holocene in age and overlies the Cuicuiltic Member (Fig. 16). The section is exposed at the bottom of an erosional “cárcava” (deep, narrow gully), and reveals the following succession. At the base, a massive, pink-to-brown lapilli-tuff with large pumice clasts may correlate with the Llano ignimbrite; because the base is not exposed, the correlation is uncertain. The ignimbrite is

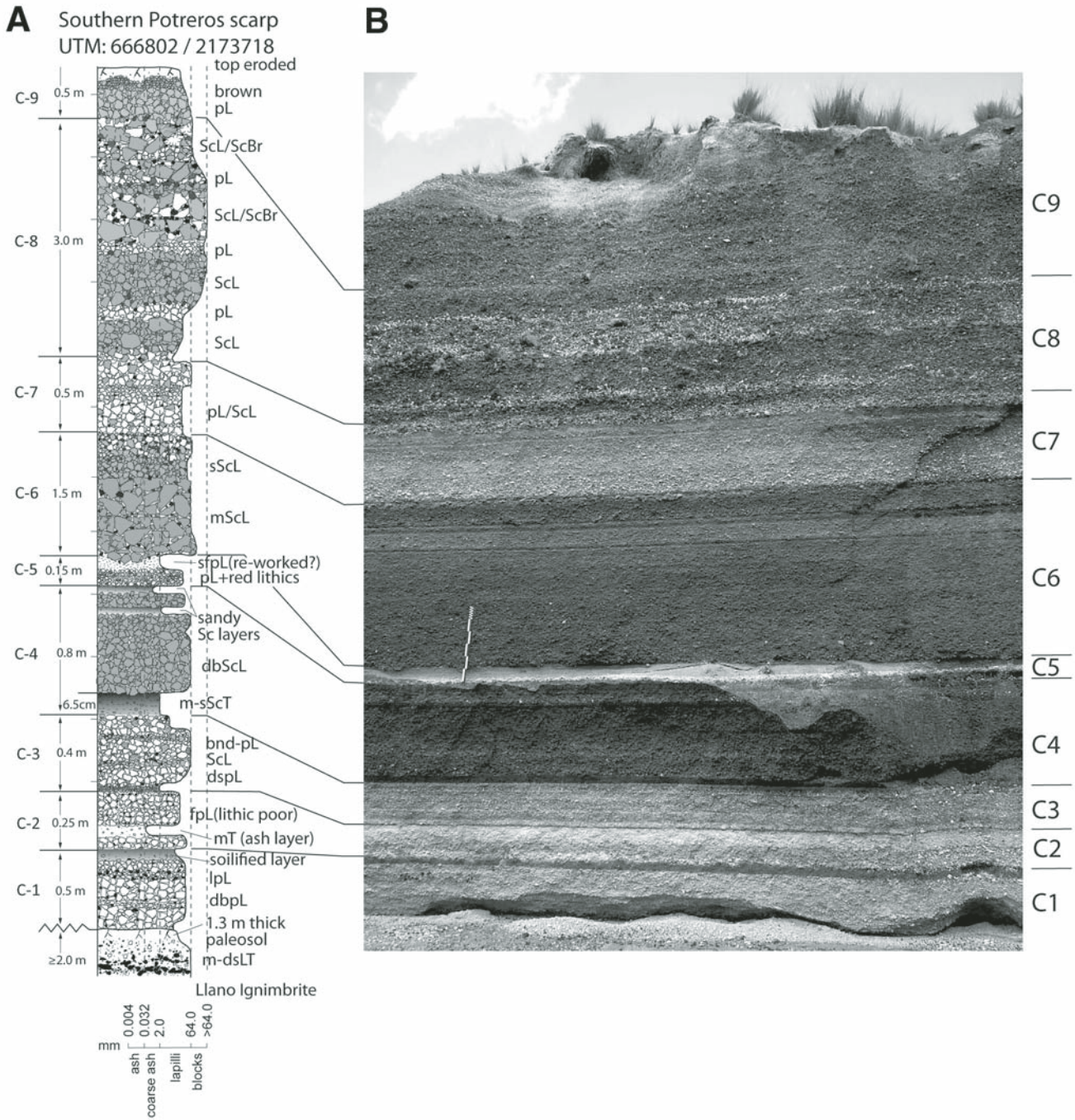


Figure 15. Stop 4: Type section of the Cuicuiltic Member, southern sector of Potrereros scarp. (A) Graphic log of the succession exposed in road cut showing all layers recognized within the eruption unit (C1 to C9) and other secondary, intermittent layers that do not correlate across the caldera. (B) Vertical exposure of the Cuicuiltic Member, with correlations between stratigraphic log and picture. Scale bar shows 0.5 m.

overlain by one or several merged paleosols, with intercalated pumice lenses that probably record eroded pumice-fall layers. The Cuicuiltic Member overlies this paleosol, with eight of its nine layers exposed (the C9 was probably eroded away at this locality). At one of the margins of the cárcava, just below the lavas, the Cuicuiltic Member appears faulted, and it is not clear

if the structure shows a lateral displacement or a slump of the near-vertical cliff due to the weight of the overlying lava. The Pájaro lavas overlie the Cuicuiltic Member unconformably, and only a slightly soilified layer is preserved at the top of C8.

The Pájaro lavas were erupted from Arenas volcano on the southwestern margin of the caldera. The flows are dacite and

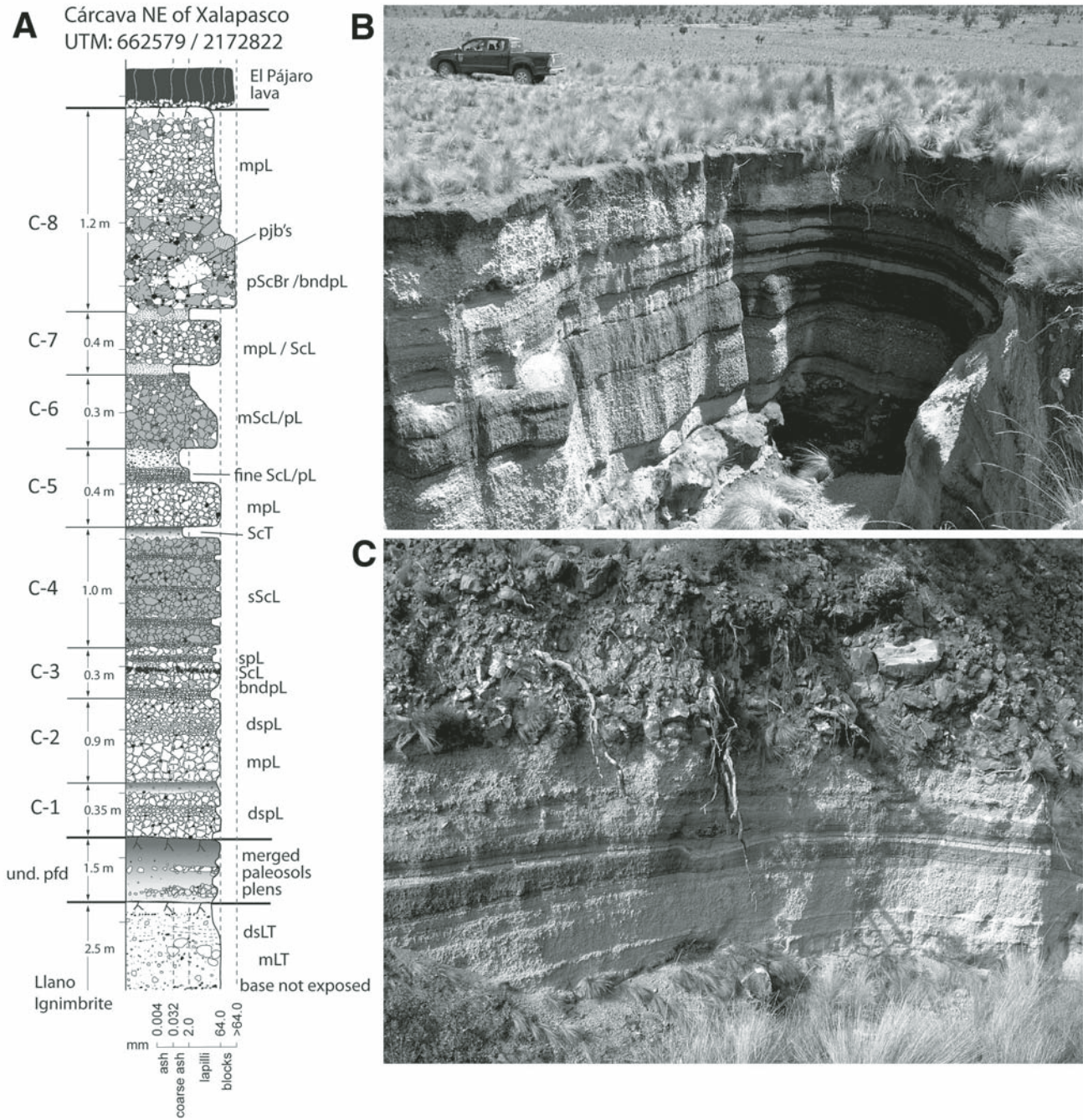


Figure 16. Stop 5: The Cuicuiltic Member north of Xalapasco crater. (A) Stratigraphic log of the succession exposed in a gully with most of its layers exposed except for C9, probably eroded. (B) View of the Cuicuiltic Member over thick paleosol that overlies a lapilli-tuff, probably the Llano ignimbrite. Truck for scale. (C) El Pájaro lavas resting unconformably on the Cuicuiltic Member, same locality as above.

pyroxene andesite and correspond to some of the youngest lava flows inside the caldera. They are less than ca. 7 ka, as they overlie the Cuicuiltic Member.

### Stop 6. Los Humeros Geothermal Wells

Visit to Los Humeros caldera interior to look at the different geothermal wells in production (Fig. 3A).

### Day 3. Road Log Begins at Hotel Cavadonga, Perote

#### Road Log, Day 3—Perote to Cerro Pizarro Dome, Cerro Pinto Tuff Ring and Dome Complex and Atexcac Maar

Return to Querétaro. Stops for Day 3 are depicted in Figure 12.

km	Directions
0.0	Meet at parking lot of the Cavadonga Hotel after breakfast at the restaurant.
0.1	Turn left (SW) and merge onto state road 140 toward Puebla.
11.0	Turn right after 11 km toward 5 de Mayo/ Tepyahualco/Cantona archaeological site and drive for other 11 km.
22.0	Arrive at Tepyahualco village.
23.0	Cross the village and drive northbound for 1 km.
26.0	Turn left at the dirt road and follow this to the quarry. Stop 7.1
28.0	Drive back to previous junction and continue toward the north to a dry stream crossing. Park the car and walk for 800 m to reach Stop 7.2. Return to the paved road connecting Tepyahualco to road 140 (Perote-Puebla), drive back until the junction to San Nicolás Pizarro village to the north, turn right and drive along a dirt road for 4.3 km crossing a dry stream. Park the car and walk upstream for 0.8 km to reach a scarp. Stop 7.3.
41.0	Drive back and return to state road 140 Perote-Puebla and turn right (southbound).
47.6	At 6.6 km is Alchichica crater, a large maar volcano with an enclosed lake.
52.6	Drive on state road 140 toward El Seco-Puebla and after 5 km turn right (west).
58.6	Pass the village Itzoteno. Cerro Pinto quarries are at 6 km; Stops 8.1, 8.2, and 8.3. Lunch time.
64.6	Drive back to main road 140 and turn right toward El Seco-Puebla.
69.6	Drive for 5 km to the junction to Guadalupe Victoria, turn left heading to San Luis Atexcac village.

70.3	After 700 m, turn right on a dirt road going toward the crater rim and park.
71.0	Walk up to reach the crater rim and walk around to the left; Stop 9.
72.0	Drive back to main road 140, turn left (SW) toward Zacatepec-Puebla.
78.0	Drive for other 6 km toward Zacatepec. We'll stop at Las Derrumbadas twin silicic domes, which show evidence of sector collapse and debris-avalanche deposits.
84.0	Pass Zacatepec village.
126.0	Take state road 136 to Huamantla-Apizaco; drive for 42 km.
153.5	Drive for 27.5 km toward Apizaco on road 136.
470.5	Drive onto road 136 until junction with toll motorway "Arco Norte" toward the northwest (Cd. Sahagún). Merge with main road 57 Mexico-Querétaro and arrive to Querétaro City (~317 km).

### Stop 7. Cerro Pizarro

#### Stop 7.1. West Side of Cerro Pizarro: Debris-Avalanche Deposits

Location: UTM 14Q 660948/2157749

This is an active quarry, and so exposures change frequently. Eastward toward Cerro Pizarro, note distinctive breach scar on the west flank of Cerro Pizarro (Fig. 17B). In this area, the debris avalanche that spread westward as the dome collapsed left a deposit that is being quarried. Features to look for are jigsaw-fit clasts (Fig. 17C), which occur only in first-stage stony rhyolite blocks, megablocks of vitrophyre, and the matrix of very finely comminuted ash between blocks. Riggs and Carrasco-Núñez (2004) estimated that the volume of collapse material was ~0.8 km<sup>3</sup> prior to erosion. To the rear of the quarry, a stratigraphic interval may be exposed that shows debris avalanche material overlain by ca. 100 ka Zaragoza ignimbrite (derived from Los Humeros caldera), in turn overlain by ca. 65 ka late-stage pyroclastic rocks that were derived from Cerro Pizarro (Fig. 8A).

#### Stop 7.2. West Side of Cerro Pizarro: Volcaniclastic Deposits and the Zaragoza Ignimbrite

Location: 14Q 661313/2158237

Drive to the north across a dry stream, park and walk into the small ravine for ~800 m to visit different exposures. The pyroclastic successions overlie volcaniclastic deposits from the partial destruction of Cerro Pizarro. The walls of the arroyo are dominantly polymitic breccias that locally show a faint stratification interpreted as debris flow reworking of the C. Pizarro debris avalanche (Riggs and Carrasco-Núñez, 2004). Large blocks of vitrophyre, similar to those in the debris-avalanche

deposit, may be exposed. Overlying these deposits are several pyroclastic layers from unknown sources, but most likely Los Humeros caldera. These are overlain by the Zaragoza ignimbrite; note the basal contact and lowest thin pumice fall layer, which is overlain by the lower rhyodacitic zone of the Zaragoza ignimbrite (Fig. 5). Apart from some minor flow units at the base, the majority of the ignimbrite comprises a single massive flow-unit. The lowermost part of this is white-cream in color, but this starts to vary 70 cm up from the base, with the appearance of the first andesitic pumice clasts. There is little evidence for any cessation of flow where the composition changes, and the unit is best interpreted as a single massive flow unit that was progressively aggraded at the base of a sustained pyroclastic density current, whose composition gradually changed with time. The protracted deposition apparently spanned the subsidence of the Los Potreros caldera, as recorded by a maxima of lithic blocks within the andesitic zone—at other locations these thicken into well-developed lithic breccias. The uppermost part of the flow unit is rhyodacitic again, showing a double compositional zonation for the Zaragoza ignimbrite as described by Carrasco-Núñez and Branney (2005). Pumice concentrations near the top are thought to record distal pumice accumulations

left as the distal limit of the current receded sourceward during waning stages of the eruption—andesitic pumices are generally absent from the uppermost parts. Discontinuous bedding in places may be the result of fluctuations in flow velocity and deposition. Circa 65 ka pyroclastic deposits from C. Pizarro are exposed locally along the top of the arroyo walls and overlie the Zaragoza ignimbrite.

### **Stop 7.3. South Side of Cerro Pizarro Dome: Vitrophyre and Early Eruptive Material**

Location: UTM 14Q 664694/2157084

The evolution of Cerro Pizarro dome is discussed above. Rocks exposed at this stop are vitrophyre and vitrophyre breccia (Fig. 17A), which are interpreted as a carapace to the original dome material (exposed in a small hill to the west of the arroyo). The “waterfall” morphology is due to the vertical orientation of the vitrophyre: to the north, a vertical succession of block-and-ash-flow deposits, 200 ka basalt, and Cretaceous limestone is exposed as far as a topographic saddle (Fig. 6). Continuing up the cone, crytodal material is exposed as far as a prominent bump on the south side of the mountain that comprises another

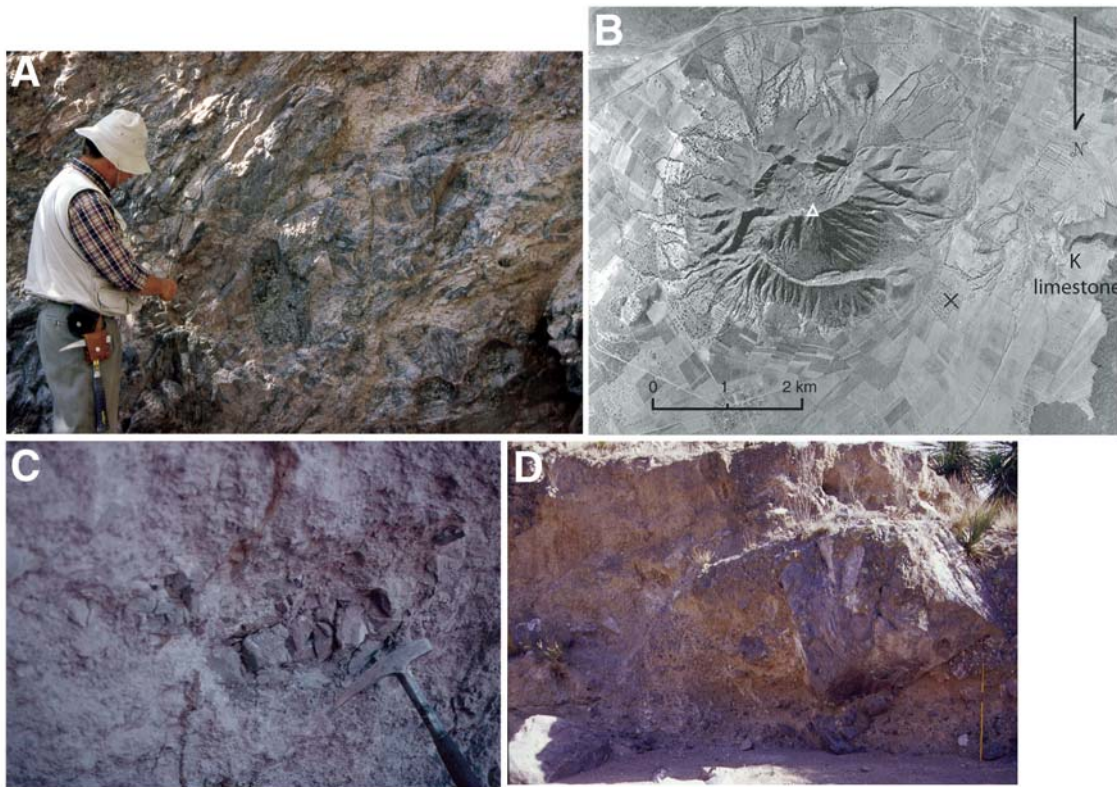


Figure 17. Stop 7. (A) Vitrophyre breccia at Stop 7.3. (B) Air photo of Cerro Pizarro. Note the open horseshoe shape of the western side of the dome; note north is to the bottom of the page. (C) Stop 7.1: Jigsaw-fracture clast of Stage 1 rhyolite. (D) Block of vitrophyre (>2 m diameter) in debris-avalanche deposit.

exposure of Cretaceous limestone (Fig. 6). Return to San Nicolás Pizarro and continue to the state road Perote-Puebla.

### Stop 8. Cerro Pinto

Location: UTM 14Q 657902/2143477

We will drive back and turn right onto the state free road Perote-Puebla. On the way to the next stop driving to the south, we will pass a spectacular maar volcano, the largest in the area, called Alchichica crater, which contains a lake. Cerro Pinto has a very irregular morphology seen from a digital elevation model (Fig. 18 inset). General geology and evolutionary stages for Cerro Pinto dome are depicted in Figure 18.

### Stop 8.1. Road to the Quarry

Location: UTM 14Q 657824/2143547

The quarry-access road approaches Cerro Pinto from the northeast. The road crosses the northern tuff ring, where it passes through surge and fallout beds from the northern ring that have lapped up against or have blanketed earlier pyroclastic deposits from the southern tuff ring (Fig. 19A). These surges were initially wet and lithic rich and were emplaced in a more turbulent depositional environment than is expressed in pyroclastic deposits elsewhere in the complex.

A small pyroclastic flow deposit exposed in the valley on the right hand side where the road bends to the south (Fig. 19B) is

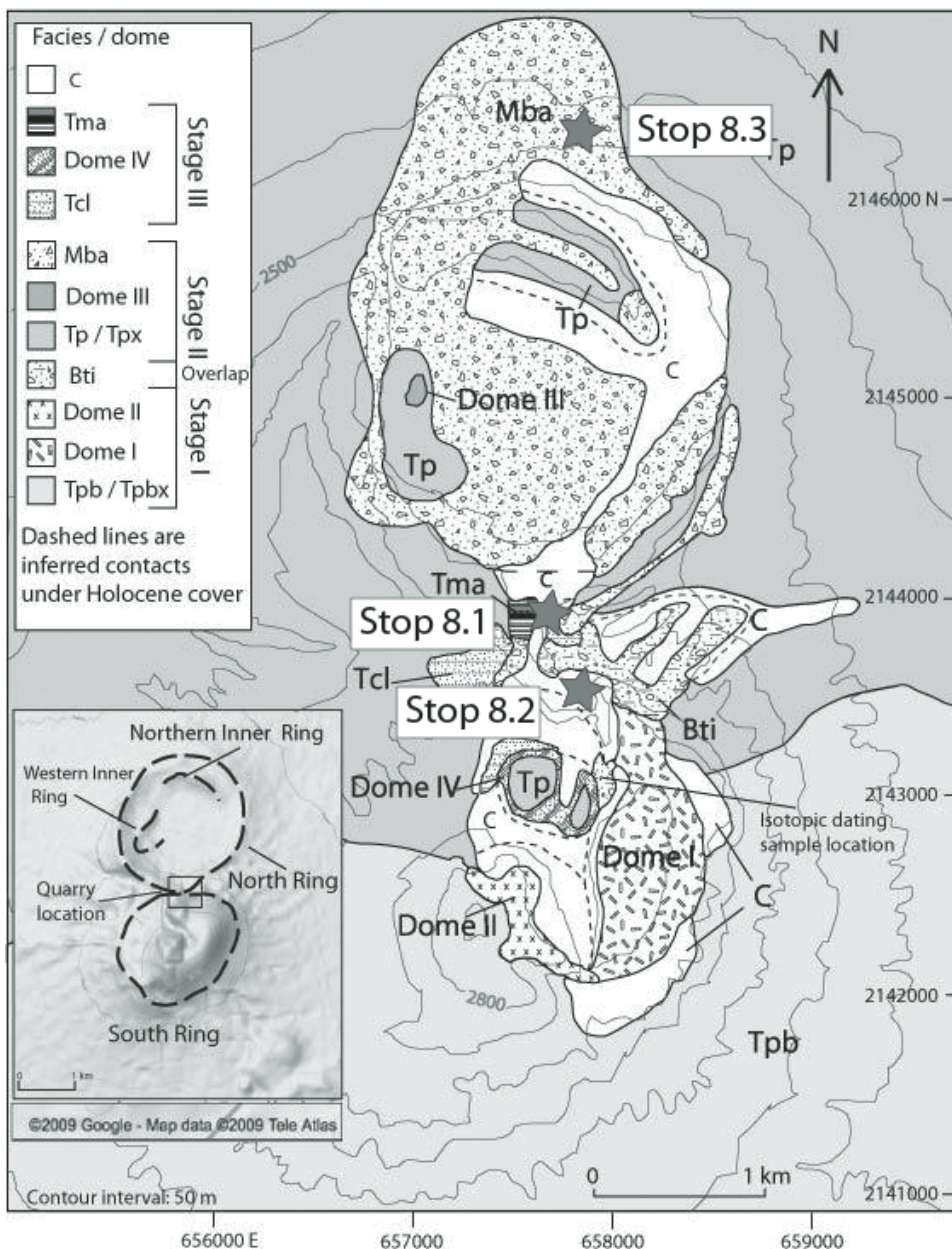


Figure 18. Facies map of Cerro Pinto showing location of local stops (stars) (Zimmer et al., 2010). Inset is a shaded relief map of Cerro Pinto identifying the ridges of the four tuff rings and the quarry location. Basic evolutionary sequence from oldest to youngest: southern tuff ring emplaced (Tpb); Dome I and Dome II emplaced within southern tuff ring; northern tuff ring emplaced (Tp); two smaller tuff rings produced within the northern tuff ring (Tp); Dome III emplaced in northern tuff ring and explosively destroyed (Mba); Dome IV emplaced in the southern tuff ring.

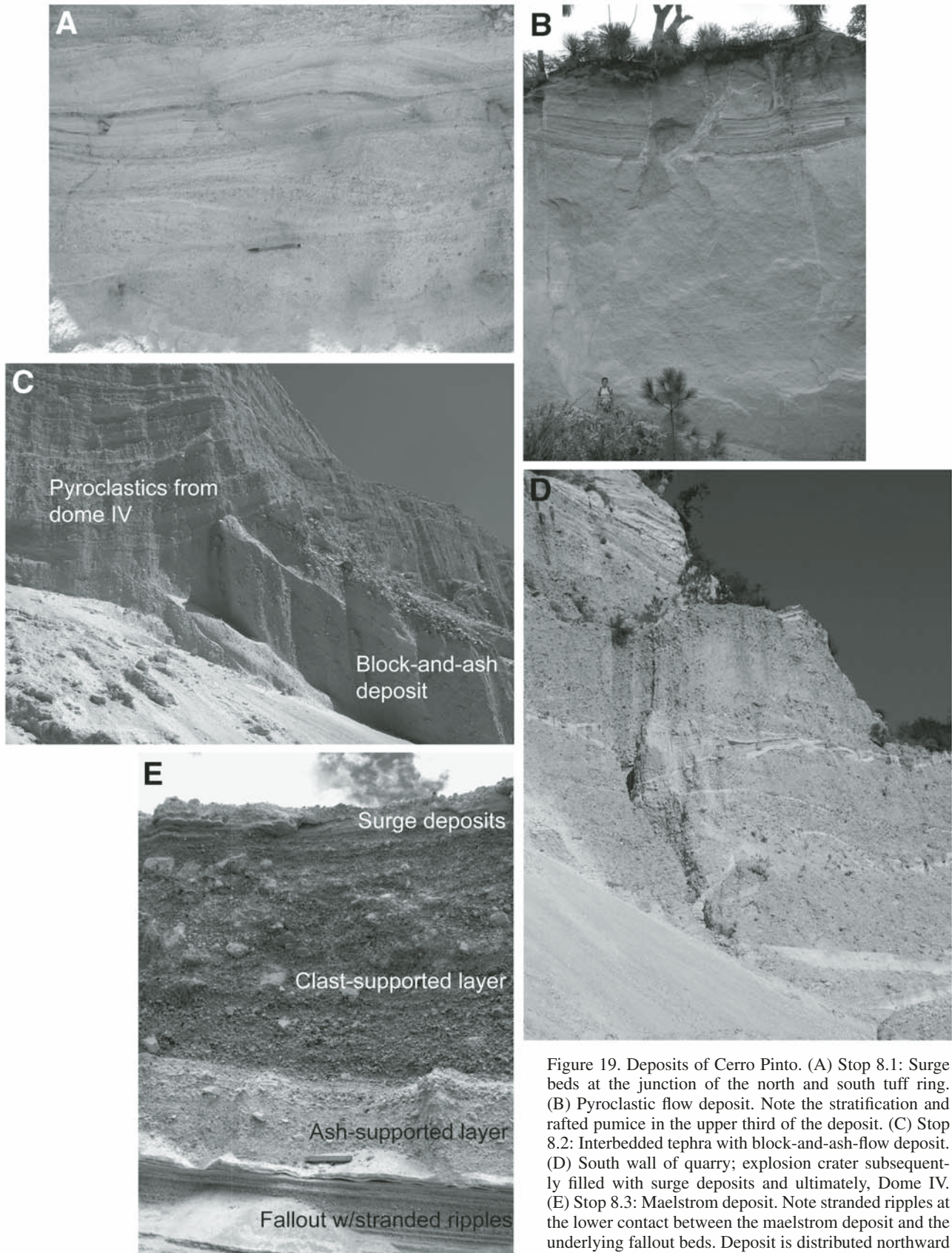


Figure 19. Deposits of Cerro Pinto. (A) Stop 8.1: Surge beds at the junction of the north and south tuff ring. (B) Pyroclastic flow deposit. Note the stratification and rafted pumice in the upper third of the deposit. (C) Stop 8.2: Interbedded tephra with block-and-ash-flow deposit. (D) South wall of quarry; explosion crater subsequently filled with surge deposits and ultimately, Dome IV. (E) Stop 8.3: Maelstrom deposit. Note stranded ripples at the lower contact between the maelstrom deposit and the underlying fallout beds. Deposit is distributed northward from dome IV (Mba; Fig. 20).

~15 m thick and has rafted pumice toward the top. The toe of the pyroclastic flow spills out into the northern tuff ring, indicating that it was deposited late in the eruptive sequence.

### **Stop 8.2. The Quarry**

Location: UTM 14Q 657902/2143477

The quarry is located just south of the junction between the northern and southern tuff rings. Mass-flow deposits from Dome I and Dome II are interbedded with fine-grained tephra (Fig. 19C); these flows were episodic, resulting from the partial collapse of the cooling domes that fill the southern tuff ring while volcanic activity continued in the northern portion of the complex. The main outcrop is capped by wet-surge deposits produced during the final stages of the eruption of the Cerro Pinto complex. Along the southern wall of the quarry, note strongly discordant bedding overlying a channel in the mass-flow deposits; Zimmer et al. (2010) suggested that this is evidence of an explosion crater that was evacuated prior to the deposition of pyroclastic deposits related to the emplacement of Dome IV (Fig. 19B).

Dome I and Dome II were emplaced in quick succession and both are composed of stony rhyolite, with Dome I having prominent flow banding. Remnants of Dome III and the entirety of Dome IV are composed of sugary white rhyolite. Modern debris-flow deposits fill many of the drainages that drain away from the quarry.

### **Stop 8.3. Flank of the Northern Ring**

Location: UTM 14Q 657913/2146285

At this site walk through an arroyo on the outer flank of the northern ring. The majority of the pyroclasts here were deposited as fallout. Brief periods of repose (minutes to hours) are indicated by the presence of stranded ripples. The top of the sequence is capped by a three-part explosion breccia that was produced during the destruction of Dome III. The breccia has an ash-rich lower bed, accounting for ~25% of the entire deposit volume, a clast-supported middle bed, accounting for around 60%, and an upper set of surge beds that account for the remaining 15%. This sequence is called the “maelstrom deposit” (Zimmer, 2007; Fig. 19E).

A maelstrom is envisaged as an environment dominated by coarse-grained fallout particles that never attained positive buoyancy in an eruption column, and so rained down in a pulsatory manner over the course of a few minutes to hours. The maelstrom deposit (Fig. 19E) is locally graded and clast supported similar to many fallout deposits, but it also has the granulometry, cross-bedding structures, out-sized clast populations and interactions with topography commonly associated with pyroclastic density-current deposits and the deposits of laterally directed blasts.

### **Stop 9. Atexcac Crater**

Location: UTM 14Q 663033/2138202

Walk to the rim for a view of the Atexcac maar crater (Fig. 10B and 10C), which is excavated into and reveals several differ-

ent rock types. The basement rocks, visible here in the western walls of the maar, are highly folded and fractured Cretaceous limestone. This rock has high fracture permeability, allowing for rapid water movement through it. Based upon lithic fragments in the Atexcac sequence, we assume that geothermally altered andesite, likely Tertiary in age, underlies the visible sequence. The limestone topographic high is covered by the deposits of a basaltic cinder cone and a basalt lava flow (dated at  $0.33 \pm 0.08$  Ma by Ar/Ar; Carrasco-Núñez et al., 2007) is present at the lake level. The relation between these two basalts is not known. Overlying this is the “Toba Café,” a brown, volcanoclastic sediment that contains volcanic-rock clasts from the Serdán-Oriental basin. The “Toba Café” represents a protracted period of aeolian and fluvial erosion and deposition. This tuff is the uppermost aquifer of the basin, and is the source of water for most of the phreatomagmatism in the area. Most maars penetrate only to this level, and Atexcac is unusual in that its explosions occurred at much greater depths. A 3.4-m-thick rhyolitic fallout tuff is intercalated within the “Toba Café,” and may represent the distal deposits from Cerro Pinto. The phreatomagmatic pyroclastic succession from Atexcac overlies the “Toba Café.”

The Atexcac phreatomagmatic deposits here are characterized by both fallout and surge deposits. Here, on the edge of the crater, they are a proximal facies, so fallout deposits are not as well sorted as those found 1 km from the vent, and the surge deposits are typically massive and lack the duneforms and bedding found farther from the vent. Lapilli tuffs and lapilli breccias are common, whereas fine-grained tuffs occur farther from the vent. Some deposits from smaller explosions provide an idea of what the medial deposits look like. Accretionally lapilli (Fig. 20) and ballistic blocks that made bomb sags in the deposits attest to the wet, soft nature of the deposits at that time and the folly of standing on the rim of a maar crater during an eruption. An obsidian breccia overlies the Atexcac sequence on the far side of the maar. This is the deposit from a collapse event at Las Derumbadas, visible behind the maar.

At this site, we will familiarize ourselves with the deposits of maar volcanoes. These deposits show evidence of condensed water being present during their emplacement, so the depositional features are those typical of sticky particles, including duneforms and impact sags. Some water may have been in gaseous form and then condensed as the currents moved from the vent, but, given the proximity to the vent here, we suspect that the liquid water was non-interactive. This water was ejected during the explosions and indicates that excess water was available in the vent area. Abundant andesite clasts in the deposits imply that explosions occurred at a depth at which the andesite was exposed. A fractured basement of andesite and limestone was likely water saturated, as may have been the thin overlying veneer of “Toba Café.” Based on the size and type of lithic and juvenile blocks, we infer that the eruption started in the SW portion of the crater and migrated to the NE, before reversing late in the eruption. It is not clear whether the eruption shut off as vents were abandoned during migration, or if the apparent migration is

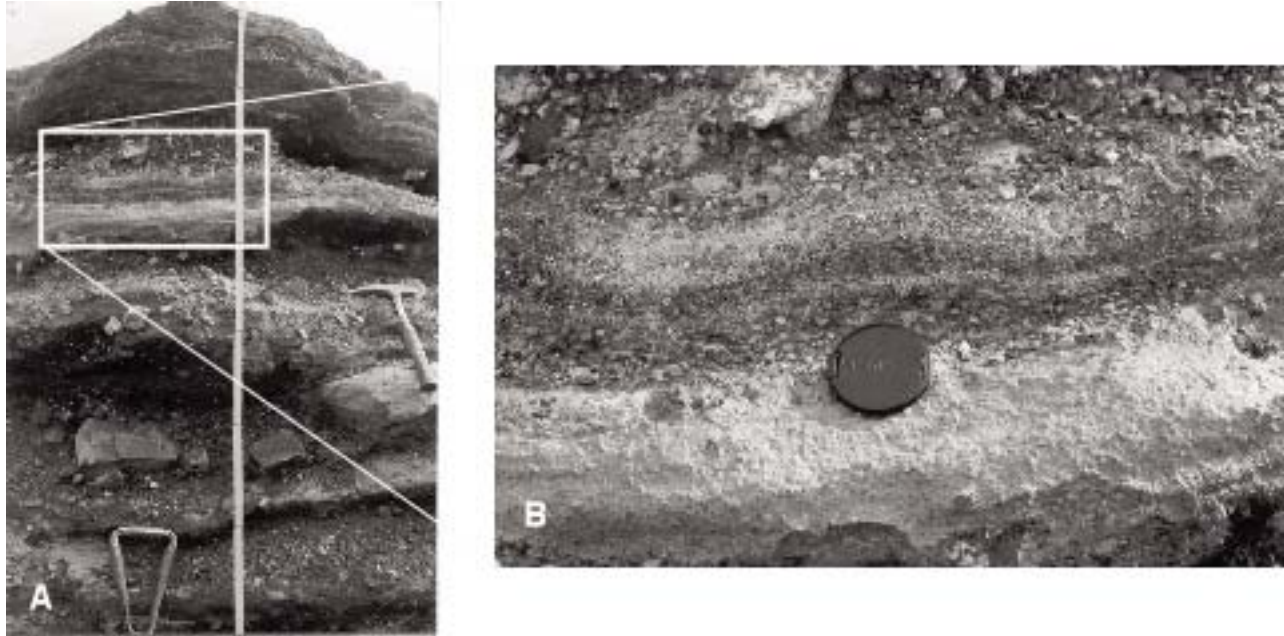


Figure 20. Stop 9. Atexcac upper section showing evidence of water influx at the latest stages of the maar-forming eruptions (Carrasco-Núñez et al., 2007).

simply due to the relative vigor of eruptions from different parts of an erupting dike.

#### ACKNOWLEDGMENTS

This field guide was funded by PAPIIT grant number IN106810 and CONACyT (temporal number 0150900). Logistical support by Centro de Geociencias. Fidel Cedillo helped us in the field around Los Humeros caldera and provided useful information related to this volcanic center. The reviewers Sergio Rodríguez and Giovanni Sosa provided useful observations that helped to improve this paper.

#### REFERENCES CITED

- Abrams, M., and Siebe, C., 1994, Cerro Xalapaxco: an unusual tuff cone with multiple explosion craters, in central Mexico (Puebla): *Journal of Volcanology and Geothermal Research*, v. 63, p. 183–199, doi:10.1016/0377-0273(94)90073-6.
- Austin-Erickson, A., 2007, Phreatomagmatic eruptions of rhyolitic magma: A case study of Tepexitl tuff ring, Serdan-Oriental Basin, Mexico [unpublished M.S. thesis]: Flagstaff, Arizona, USA, Northern Arizona University, 194 p.
- Austin-Erickson, A., Ort, M.H., and Carrasco-Núñez, G., 2011, Rhyolitic phreatomagmatism explored: Tepexitl tuff ring (Eastern Mexican Volcanic Belt): *Journal of Volcanology and Geothermal Research*, v. 201, p. 325–341, doi:10.1016/j.jvolgeores.2010.09.007.
- Blake, S., and Ivey, G.N., 1988, Density and viscosity gradients on zoned magma chambers, and their influence on withdrawal dynamics: *Journal of Volcanology and Geothermal Research*, v. 30, p. 200–229.
- Branney, M.J., and Kokelaar, B.P., 1997, Giant bed from a sustained catastrophic density current flowing over topography: Acatlán Ignimbrite, Mexico: *Geology*, v. 25, p. 115–118, doi:10.1130/0091-7613(1997)025<0115:GBFASC>2.3.CO;2.
- Branney, M.J., and Kokelaar, B.P., 2002, Pyroclastic density currents and the sedimentation of ignimbrites: *Geological Society of London Memoir* 27, 152 p.
- Brown, R.J., and Branney, M.J., 2004, Event-stratigraphy of a caldera-forming ignimbrite eruption on Tenerife: the 273 ka Poris Formation: *Bulletin of Volcanology*, v. 66, p. 392–416.
- Bryan, S.E., Martí, J., and Cas, R.A.F., 1998, Stratigraphy of the Bandas del Sur Formation: An extracaldera record of Quaternary phonolitic explosive volcanism from the Las Cañadas edifice, Tenerife (Canary Islands): *Geological Magazine*, v. 135, p. 605–636, doi:10.1017/S0016756897001258.
- Carrasco-Núñez, G., 2000, Structure and proximal stratigraphy of Citlaltépetl Volcano (Pico de Orizaba), Mexico, in Delgado-Granados, H., Aguirre-Díaz, G., Stock, J., eds., *Cenozoic Volcanism and Tectonics of Mexico: Geological Society of America Special Paper* 334, p. 247–262, doi:10.1130/0-8137-2334-5.247.
- Carrasco-Núñez, G., and Branney, M.J., 2005, Progressive assembly of a massive layer of ignimbrite with normal-to-reverse compositional zoning: the Zaragoza ignimbrite of central Mexico: *Bulletin of Volcanology*, v. 68, p. 3–20, doi:10.1007/s00445-005-0416-8.
- Carrasco-Núñez, G., and Riggs, N., 2008, Polygenetic nature of a rhyolitic dome and implications for hazard assessment: Cerro Pizarro volcano, Mexico: *Journal of Volcanology and Geothermal Research*, v. 171, p. 307–315, doi:10.1016/j.jvolgeores.2007.12.002.
- Carrasco-Núñez, G., Ort, M.H., and Romero, C., 2007, Evolution and hydrological conditions of a maar volcano (Atexcac crater, Eastern Mexico), in Martin, U., Németh, K., Lorenz, V., White, J., eds., *Maar-diatreme volcanism and associated processes: Journal of Volcanology and Geothermal Research*, v. 159, p. 179–197.
- Carrasco-Núñez, G., Gómez-Tuena, A., and Lozano, L., 1997, Geologic map of Cerro Grande volcano and surrounding area, Central Mexico: *Geological Society of America Map and Chart Series* 81, 10 p.
- Carrasco-Núñez, G., Díaz-Castellón, R., Siebert, L., Hubbard, B., Sheridan, M.F., and Rodríguez, S.R., 2006, Multiple edifice-collapse events in the Eastern Mexican Volcanic Belt: the role of sloping substrate and implications for hazard assessment, in Tibaldi, A., and Lagmay, A., eds., *The effects of basement structural and stratigraphic heritages on volcano behaviour: Journal of Volcanology and Geothermal Research*, v. 158, p. 151–176.
- Carrasco-Núñez, G., Siebert, L., Díaz-Castellón, R., Vázquez-Selem, L., and Capra, L., 2010, Evolution and hazards of a long-quiet compound

- shield-like volcano: Cofre de Perote, Eastern Trans-Mexican Volcanic Belt: *Journal of Volcanology and Geothermal Research*, v. 197, p. 209–224, doi:10.1016/j.jvolgeores.2009.08.010.
- Carrasco-Núñez, G., McCurry, M., Branney, M.J., Norry, M., and Willcox, C., 2012, Complex magma mixing, mingling, and withdrawal associated with an intraplinian ignimbrite eruption at a large silicic caldera volcano: Los Humeros of central Mexico: *Geological Society of America Bulletin*, doi:10.1130/B30501.1 (in press).
- Dávila-Harris, P., and Carrasco-Núñez, G., 2010, La toba Cuicuiltic (30 ka): erupción sub-Pliniana más joven en la caldera de Los Humeros y volcanismo bimodal contemporáneo asociado: *Geos*, v. 30-1, p. 103.
- Ferrari, L., López-Martínez, M., Aguirre-Díaz, G., and Carrasco-Núñez, G., 1999, Spacetime patterns of Cenozoic arc volcanism in Central Mexico: from the Sierra Madre Occidental to the Mexican Volcanic Belt: *Geology*, v. 27, no. 4, p. 303–306, doi:10.1130/0091-7613(1999)027<0303:STPOCA>2.3.CO;2.
- Ferriz, H., and Mahood, G., 1984, Eruption rates and compositional trends at Los Humeros volcanic center, Puebla, Mexico: *Journal of Geophysical Research*, v. 89, B10, p. 8511–8524, doi:10.1029/JB089iB10p08511.
- Gasca-Durán, A., 1981, Génesis de los lagos-cráter de la cuenca de Oriental: *Colección Científica Prehistórica*, v. 98, 57 p.
- Gómez-Tuena, A., and Carrasco-Núñez, G., 2000, Cerro Grande volcano: the evolution of a Miocene stratocone in the early trans-Mexican Volcanic Belt: *Tectonophysics*, v. 318, p. 249–280, doi:10.1016/S0040-1951(99)00314-5.
- Lorenz, V., 1986, On the growth of maar and diatremes and its relevance to the formation of tuff rings: *Bulletin of Volcanology*, v. 48, p. 265–274, doi:10.1007/BF01081755.
- McConnell, S., 2004, An analytical approach to the interpretation of complex dome formation, Cerro Pizarro, Mexico [unpublished M.S. thesis]: Flagstaff, Arizona, USA, Northern Arizona University, 226 p.
- Negendank, J., Emmermann, R., Krawczyk, R., Mooer, F., Tobschall, H., and Werle, D., 1985, Geological and geochemical investigations on the eastern TMV: *Geofísica International*, v. 24, p. 477–575.
- Ordóñez, E., 1905, Los xalapaxcos del estado de Puebla: *Instituto de Geología, México*, p. 350–393.
- Ordóñez, E., 1906, Los xalapaxcos del estado de Puebla: *Instituto de Geología, México*, p. 350–393 2a parte.
- Ort, M.H., and Carrasco-Núñez, G., 2009, Lateral vent migration during phreatomagmatic and magmatic eruptions at Tecuítlapa Maar, east-central Mexico: *Journal of Volcanology and Geothermal Research*, v. 181, p. 67–77, doi:10.1016/j.jvolgeores.2009.01.003.
- Riggs, N.R., and Carrasco-Núñez, G., 2004, Evolution of a complex, isolated dome system, Cerro Pizarro, central Mexico: *Bulletin of Volcanology*, v. 66, p. 322–335, doi:10.1007/s00445-003-0313-y.
- Rodríguez-Elizarrarás, S.R., 2005, Geology of the Las Cumbres Volcanic Complex, Puebla and Veracruz states, Mexico: *Revista Mexicana de Ciencias Geológicas*, v. 22, p. 181–198.
- Romero, C., 2000, Estratigrafía del cráter Atexcac [unpub. Bch. thesis]: Engineering Fac., Universidad Nacional Autónoma de México, 98 p.
- Siebe, C., Macías, J.L., Abrams, M., Rodríguez-Elizarrarás, S., Castro, R., and Delgado, H., 1995, Quaternary explosive volcanism and pyroclastic deposits in east central Mexico: Implications for future hazards, in Chacko, J., ed., *Guidebook for the 1995 Annual Meeting of the Geological Society of America*, New Orleans, Louisiana, p. 1–47.
- Siebert, L., and Carrasco-Núñez, G., 2002, Late-Pleistocene to precolumbian behind-the-arc mafic volcanism in the eastern Mexican Volcanic Belt; implications for future hazards: *Journal of Volcanology and Geothermal Research*, v. 115, p. 179–205, doi:10.1016/S0377-0273(01)00316-X.
- Viniegra, F., 1965, Geología del Macizo de Teziutlán y la Cuenca Cenozoica de Veracruz: *Boletín Asociación Mexicana Geólogos Petroleros*, v. 17, p. 101–163.
- Willcox, C.P., 2011, Eruptive, magmatic and structural evolution of a large explosive caldera volcano: Los Humeros, Central Mexico [unpublished Ph.D. thesis]: University of Leicester, Leicester, U.K.
- Yáñez, C., and García, S., 1982, Exploración de la región geotérmica Los Humeros–Las Derrumbadas, estados Puebla y Veracruz: *Comisión Federal de Electricidad, México*, v. 29, p. 98.
- Zimmer, B.W., 2007, Eruptive variations during the emplacement of Cerro Pinto dome complex, Puebla, Mexico [M.S. thesis]: Northern Arizona University, 119 p.
- Zimmer, B., Riggs, N.R., and Carrasco-Núñez, G., 2010, Evolution of tuff ring-dome complex: the case study of Cerro Pinto, eastern Trans-Mexican Volcanic Belt: *Bulletin of Volcanology*, v. 72, p. 1223–1240, doi:10.1007/s00445-010-0391-6.

